

***A Novel Approach for Computing Particle Collection
Efficiency of Electrostatic Scrubber***

*Thesis submitted in partial fulfilment of the requirement for the award of
degree of*

***Master of Engineering
in
Electronics Instrumentation and Control***



Submitted By:

Kriti Jain
(800951015)

Under the Supervision of:

Dr. Mandeep Singh
*Assistant Professor
EIED*

JULY 2011

***ELECTRICAL AND INSTRUMENTATION ENGINEERING DEPARTMENT
THAPAR UNIVERSITY
PATIALA – 147004***

Declaration

I hereby declare that the report entitled "A Novel Approach for Computing Particle Collection Efficiency of Electrostatic Scrubber", is an authentic record of my own work carried out as a requirement for the award of degree of M.E. (Electronic Instrumentation & Control) at Thapar University, Patiala, under the guidance of **Dr. Mandeep Singh (AP, EIED)** during January to July 2011.

Kriti

Kriti Jain

Roll No. : 800951015

Date: 12 July, 2011

It is certified that the above statement made by the student is correct to the best of my knowledge and belief.

(Signature)

Dr. Mandeep Singh

Assistant Professor, EIED
Thapar University, Patiala

Countersigned by:

S. Ghosh
14/7/11

Dr. Smarajit Ghosh

Professor & Head, EIED
Thapar University, Patiala.

(Signature)

Dr. S.K. Mohapatra

Dean of Academic Affairs
Thapar University, Patiala.

Acknowledgements

The real spirit of achieving a goal is through the way of excellence and austere discipline. I would have never succeeded in completing my task without the cooperation, encouragement and help provided to me by various personalities.

*With deep sense of gratitude I express my sincere thanks to my esteemed and worthy supervisor, **Dr. Mandeep Singh, Assistant Professor, Department of Electrical & Instrumentation Engineering, Thapar University, Patiala**, for his valuable guidance in carrying out this work under his effective supervision, encouragement, enlightenment and cooperation.*

*I shall be failing in my duties if I do not express my deep sense of gratitude towards **Dr. Smarajit Ghosh, Professor & Head of the department of Electrical & Instrumentation Engineering, Thapar University, Patiala** who has been a constant source of inspiration for me throughout this work.*

I am also thankful to all the staff members of the Department for their full cooperation and help.

My greatest thanks are to all who wished me success especially my parents, family and friends who encouraged and supported at every point of time. Above all I render my gratitude to the ALMIGHTY who bestowed self-confidence, ability and strength in me to complete this work.

Place: Thapar University, Patiala


Kriti Jain

Date: 12 July, 2011

Roll No. 800951015

One of the major causes of air pollution is the presence of particulate matter such as dust, mist, smoke, or vapour in the atmosphere in amounts that may be harmful to human, plant or property. Particles which are submicron in size tend to remain entrained in the gas stream. To collect particles of such small size with high efficiency electrostatic charging of the particles is done. The electrostatic scrubber uses charged collector droplets to collect the dust particles of same or opposite polarity. Following Coulomb's Law, the small particles get attracted towards the water droplets. These collector droplets, after the deposition of the dust particles, are removed from the apparatus and simultaneously fresh droplets enter the system. This electrostatic system shows far better performance as compared to other conventional scrubbers. The main advantages of using an electrostatic scrubber are low water consumption, low power consumption, low operation cost and low wear and tear.

Thus in past, several authors have simulated and studied the performance and collection efficiency of the system using stream function and finite element method, which makes it difficult to understand and calculate the path followed by the dust particles.

Thus here we use an alternate method of plotting these trajectories and thus calculating the dust collection efficiency in a simplified manner using Runge-Kutta method. These trajectories are plotted by calculating the co-ordinates of the dust particle and the collector droplet at each instant of time for different set of conditions. And the collection efficiency is calculated by taking the ratio of number of particles depositing on the collector to the number of particles entering the system. This collection efficiency is studied with respect to various parameters, such as collector radius, Coulomb number, Stokes number, keeping all others constant. The graphs showing these particle trajectories and collection efficiency relations have been presented.

Organization of Thesis

The complete project thesis is divided into seven chapters as follows.

The first chapter introduces different types of scrubbers, explains working of electrostatic precipitator and finally explains the electrostatic scrubber.

The second chapter discusses the basics of the concepts used such as Coulomb's law, Stokes law, different forces on a particle, Reynolds number and Runge-Kutta algorithm.

The third chapter tells about the work that has been already carried out in this field.

The fourth chapter formulates the problem.

The fifth chapter gives the detailed description of proposed solution with an algorithm and implementation of various tools of application software.

The sixth chapter shows the result obtained in the tabular form and discussion over the result.

In the seventh chapter thesis concluded with future scopes.

Table of Contents

| Item Description | Page No. |
|---|-----------------|
| Declaration | ii |
| Acknowledgement | iii |
| Abstract | iv |
| Organization of Thesis | v |
| Table of Contents | vi |
| List of Figures | ix |
| List of Tables | xi |
| Nomenclature | xii |
| | |
| Chapter 1: INTRODUCTION | 1 |
| 1.1 Air Pollution Control | 1 |
| 1.2 Scrubber Types | 2 |
| 1.2.1 Plate Type Scrubber | 2 |
| 1.2.2 Venturi Scrubber | 3 |
| 1.2.3 Cyclonic Spray Scrubber | 3 |
| 1.2.4 Electrostatic Scrubber | 4 |
| 1.2.5 Fabric Filter | 4 |
| 1.3 Electrostatic Precipitator | 5 |
| 1.4 Theory of Precipitation | 6 |
| 1.4.1 Charging | 6 |
| 1.4.1.1 Corona Discharge | 7 |
| 1.4.1.2 Ionization of Gas Molecules | 9 |

| | |
|---|-----------|
| 1.4.1.3 Charging of Particles..... | 10 |
| 1.4.1.4 Particle Charging Mechanisms | 11 |
| 1.4.2 Electric Field Strength | 13 |
| 1.4.3 Particle Charging | 14 |
| 1.4.4 Particle Removal..... | 15 |
| 1.5 Steps for Working of ESP..... | 16 |
| 1.6 Types of Electrostatic Precipitator | 17 |
| 1.7 Electrostatic Scrubber | 17 |
| 1.7.1 Introduction..... | 17 |
| 1.7.2 Basic Working Principle | 17 |
| 1.7.3 Difference between Electrostatic Scrubber and ESP | 19 |
| 1.7.4 Advantages and Disadvantages..... | 19 |
| 1.7.5 Particle Deposition Mechanisms..... | 19 |
| 1.7.6 Some Important Features | 20 |
| | |
| Chapter 2: CONCEPT REVIEW..... | 22 |
| 2.1 Coulomb's Law..... | 22 |
| 2.2 Stoke's Law | 23 |
| 2.3 Thermophoresis Force | 25 |
| 2.4 Diffusionphoresis Force..... | 25 |
| 2.5 Image Force | 25 |
| 2.6 Reynolds Number | 26 |
| 2.7 Navier-Stokes Equation | 27 |
| 2.8 Numerical Algorithm | 28 |
| 2.8.1 Principle | 29 |
| 2.8.2 Euler's Method..... | 30 |

| | |
|---|-----------|
| 2.8.3 Second-Order Runge-Kutta Method | 31 |
| 2.8.4 Fourth-Order Runge-Kutta Method | 32 |
| 2.9 MATLAB Functions | 33 |
| Chapter 3: LITERATURE REVIEW | 34 |
| Chapter 4: PROBLEM FORMULATION | 42 |
| Chapter 5: METHODOLOGY | 44 |
| 5.1 Mathematical model..... | 44 |
| 5.2 Idealizing Assumptions..... | 44 |
| 5.3 Theoretical Background..... | 45 |
| 5.4.1 Particle Trajectory..... | 45 |
| 5.4.2 Droplet Trajectory | 49 |
| 5.4 Numerical Simulation Algorithm | 51 |
| Chapter 6: RESULTS AND DISCUSSION..... | 52 |
| 6.1 Particle Trajectory..... | 52 |
| 6.2 Collection Efficiency | 56 |
| Chapter 7: CONCLUSION AND FUTURE SCOPE | 65 |
| 7.1 Conclusion | 65 |
| 7.2 Future Scope | 66 |
| REFERENCES | 67 |
| APPENDIX A..... | 70 |
| PUBLICATIONS..... | 74 |

List of Figures

| | |
|---|----|
| Figure 1.1: Typical dry electrostatic precipitator..... | 6 |
| Figure 1.2: ESP electric field | 7 |
| Figure 1.3: Corona generation | 8 |
| Figure 1.4: Avalanche multiplication of gas molecules..... | 8 |
| Figure 1.5: Negative gas ions formed in the inter-electrode Region | 9 |
| Figure 1.6: Particle charging..... | 11 |
| Figure 1.7: Field charging..... | 12 |
| Figure 1.8: Spark generation profile | 14 |
| Figure 1.9: Particle collection at collection electrode..... | 15 |
| Figure 1.10: Schematic Diagram of Electrostatic Scrubber | 18 |
| | |
| Figure 6.1: Particle trajectories in presence of oppositely charged collector when $K_c=-10$, $St=0.1$ and $R_c=1$ | 53 |
| Figure 6.2: Particle trajectories in presence of oppositely charged collector when $K_c=-100$, $St=0.1$ and $R_c=1$ | 53 |
| Figure 6.3: Particle trajectories in presence of oppositely charged collector when $K_c=-10$, $St=1$ and $R_c=1$ | 54 |
| Figure 6.4: Particle trajectories in presence of oppositely charged collector when $K_c=-100$, $St=1$ and $R_c=1$ | 54 |
| Figure 6.5: Particle trajectories in presence of oppositely charged collector when $K_c=-10$, $St=10$ and $R_c=1$ | 55 |

| | |
|---|----|
| Figure 6.6: Particle trajectories in presence of oppositely charged collector | |
| when $K_c=-100$, $St=10$ and $R_c=1$ | 55 |
| Figure 6.7(a): Radius Vs Collection efficiency at $St=0.1$ | 57 |
| Figure 6.7(b): Inverse of Radius Vs Collection efficiency at $St = 0.1$ | 57 |
| Figure 6.8: Radius Vs Collection efficiency at $St=0.1$, extended graph..... | 58 |
| Figure 6.9: Radius Vs Collection efficiency at $St=10$ | 59 |
| Figure 6.10: Radius Vs Collection efficiency at $St=0.1$, $K_c = -10$ | 60 |
| Figure 6.11(a): Coulomb number Vs Collection efficiency at $St=0.1$, $R_c=1$ | 61 |
| Figure 6.11(b): Coulomb number Vs square of Collection efficiency | |
| at $St=0.1$, $R_c=1$ | 62 |
| Figure 6.12: Comparing Collector radius Vs Collection efficiency | |
| at $St=0.1$, 1 and 10 | 63 |
| Figure 6.13: Stokes number Vs Collection efficiency | 64 |

List of Tables

| | |
|---|----|
| Table 1.1: Comparison of different scrubbers..... | 5 |
| Table 2.1: MATLAB command recommendations..... | 33 |

Nomenclature

| | |
|-------------|--|
| C_c | Cunningham slip correction factor |
| C_d | Drag coefficient depending on Reynolds number of the particle |
| C_x | Drag coefficient depending on Reynolds number of the collector |
| \vec{F}_A | Aerodynamic drag |
| \vec{F}_B | Basset force |
| \vec{F}_D | Diffusiophoresis force |
| \vec{F}_e | Electrical force |
| \vec{F}_T | Thermophoresis force |
| \vec{F}_S | Stokes drag force |
| \vec{F}_g | Gravitational force |
| g | Gravitational field (standard average value) |
| G | Non-dimensional gravity force |
| Kc | Coulombs number |
| m_p | Particle mass |
| m_c | Collector mass |
| Q_c | Charge on the particle |
| Q_p | Charge on the particle |
| r | Distance between particle and the droplet |
| Re_p | Reynolds number based on the particle |
| Re_c | Reynolds number based on the collector |
| R_p | Radius of particle |
| R_c | Radius of collector |
| St | Stokes number |
| \vec{u} | Gas velocity in undisturbed region (far from collector) |
| u_0 | Initial velocity of the gas in undisturbed region |
| \vec{v}_c | Droplet velocity |
| \vec{w} | Particle velocity |
| x | Horizontal co-ordinate of dist between particle and collector |
| y | Vertical co-ordinate of dist between particle and collector |

Greeks

| | |
|-----------------|---|
| ε_c | Relative permittivity of the collector |
| ε_p | Relative permittivity of the collectors |
| η_g | Gas viscosity |
| ρ_g | Gas density |
| ρ_p | Particle density |
| ρ_c | Collector density |

CHAPTER 1

INTRODUCTION

1.1 Air Pollution Control

Air pollution – the presence of one or more contaminants such as dust, mist, odour, smoke, fumes, gases or vapour in the atmosphere in quantities/ amounts that may be injurious to human, plant or property. The best control measure for air pollution is prevention. However, as long as fossil fuels are used for energy such as in thermal power-plants, automobiles, textile industries, etc. there will be air pollution. To reduce future impacts we need to control air pollution. Thus to control air pollution, we need to apply control programs. Thus for this, environmental regulations are becoming more and more strict all over the world.

Many different types of control devices/de-dusting systems are now installed depending upon the situation to achieve low dust emissions. These can either used to destroy contaminants or remove them from an exhaust stream before they are emitted into the atmosphere. Using a single control device leads to high dust emissions due to low efficiency and inability of the device since it responds slowly to the changing conditions of the process. Choosing a right equipment type and design requires sophisticated methods of selection as well as provision for efficiently operating those components adapted to the existing construction, operating and environmental requirements. Thus we need complete process knowledge and advanced analytical tools for efficient system design and selection.

Most air filtration systems are designed to handle only one particular pollutant, while some filtration systems can handle two or more pollutants /contaminants simultaneously. Scrubbers are one of the primary devices that control gaseous emissions. Scrubbers are air pollution control devices that can be used to selectively remove or absorb particles (solid or liquid) and/ or gases or chemicals from exhaust streams before they are released into the air.

There are two main categories of scrubbing:

- Wet scrubbing
- Dry scrubbing

In dry scrubbing, an alkaline reagent is injected into the gas stream while preventing the gas from being saturated with water vapours. In wet scrubbing the most common choice of absorbent liquor is water. In special cases any other relatively non-volatile liquid may be used as the absorbent.

1.2 Scrubber Types

Some of the most commonly used scrubber types are as following:

1.2.1 Plate Type Scrubber

A plate-type scrubber consists of a hollow vertical tower with one or more plates or trays mounted transversely in the tower. Gas comes in from the bottom of the tower, and then passes through perforations, valves, slots, or other openings in each plate and finally exits from the top. Liquid is usually introduced at the top plate which flows successively across each plate as it moves downwards to the liquid exit at the bottom. Gas passing through the openings in each plate mixes with the liquid flowing over each plate.

The gas and liquid contact allows the mass transfer or particle removal for which the plate scrubber has been designed. These scrubbers have the ability to remove gaseous pollutants to any desired concentration level using a sufficient number of plates are used. Plates, or trays, can be designed in a variety of ways. The ones most commonly used for industrial sources are the sieve, impingement, bubble-cap, and valve.

1.2.2 Venturi Scrubber

A venturi scrubber consists of three sections: a converging section, a throat section, and a diverging section. The exhaust stream enters from the converging section and as the area decreases gas velocity increases. Liquid can be introduced either at the throat or at the entrance to the converging section.

The exhaust gas, forced to move at extremely high velocities in the small throat section, shears the liquid from its walls, thus producing an enormous number of very tiny liquid droplets. Particle and gas removal occurs in the throat section as the exhaust stream mixes with the fog of tiny liquid droplets. The exhaust stream finally exits through the diverging section. Here it is forced to slow down. Venturi scrubbers can be used to collect both particulate as well as gaseous pollutants, but these are more effective in removing particles as compared to gaseous pollutants. Liquid can be injected at the converging section or at the throat section.

Thus, the liquid coats the venturi throat making it very effective for handling hot, dry exhaust gases that contains dust particles. Otherwise, the dust would have a tendency to cake on a dry throat. These venture scrubbers are sometimes referred to as having a wetted approach. The gas velocity can be controlled by adjusting the area of the venturi throat. Due to the absence of moving parts, scrubbers of this type are especially suitable for the collection of sticky particles.

1.2.3 Cyclonic Spray Scrubbers

Cyclonic spray scrubbers use the features of both the dry cyclone and the spray chamber to collect the pollutants. Generally, the exhaust gas enters the chamber tangentially then swirls through the chamber in a corkscrew motion and finally exits. At the same time, liquid is also sprayed inside the chamber. As the exhaust gas swirls around the chamber, pollutants impact on liquid droplet and get captured, then they are thrown to the walls and finally washed back down and out. In the irrigated cyclone, the exhaust gas enters from the top of the scrubber into the water sprays. The exhaust gas is forced to swirl downward, then change directions, and finally return upward in a tighter spiral.

The liquid droplets produced to capture the pollutants are eventually thrown to the side walls and are carried out of the collector chamber. The gas with reduced pollutants leaves through the top of the chamber. The cyclonic spray scrubber forces the exhaust gas up through the chamber from a bottom tangential entry. Liquid sprayed from nozzles on a centre post is directed towards the chamber walls and through the swirling exhaust gas. In the irrigated cyclone, liquid first captures the pollutant then is forced to the walls and finally is washed out. The cleaned gas continues upward, exiting through the top of the chamber.

1.2.4 Electrostatic Precipitator

An electrostatic precipitator is a device which removes the dust particles from a polluted gas stream. It accomplishes particle separation by the use of an electric field which imparts a positive or negative charge to the particle. The charged particle is then attracted to an oppositely charged plate or a tube and is finally removed from the collection surface to a hopper by either vibrating or rapping the collection surface.

Electrostatic precipitators are one of the most widely used particulate control devices. They are used to control particulate emissions from the electric utility industry, industrial boiler plants, municipal incinerators, the non-ferrous, iron and steel, chemical, cement, and paper industries.

1.2.5 Fabric Filter

Fabric filters are used to remove the dust particles from a dust filled gas stream. They are made of a woven or felted material in the shape of a cylindrical bag or a flat supported envelope. These are contained in a housing which has gas inlet and outlet connections, a dust collection hopper, and a cleaning mechanism for periodic removal of the collected dust from the fabric. In operation, dust laden gas flows through the filters, this removes the dust particles from the gas stream [1].

Table 1.1: Comparison of different scrubbers

| S. No. | TYPE | Advantages | Disadvantages |
|--------|---------------------|--|--|
| 1. | ESP | Improved efficiency for submicron sized particles, low maintenance cost | No plugging problem, high capital cost, corrosion, high voltage required |
| 2. | Venturi scrubber | Best for cool and moist stream since there is no plugging problem, no scaling problem, can be designed for high efficiency as 99% for 0.5-2 μm size particles | High operating cost, high wear/abrasion due to high gas velocities. |
| 3. | Cyclonic scrubber | Show efficiency of 90% for μm size particles | Nozzle plugging, corrosion, erosion |
| 4. | Plate-type scrubber | Show high efficiency for soluble pollutants, desulfurization | Plugging problem, scalp build up problem, liquid-gas distribution problem, flooding, weeping |
| 5. | Fabric Filter | Low installation and maintenance cost, easy operation, no corrosion | Plugging, fabric bags tend to burn or melt at extremely high temperatures |

1.3 Electrostatic Precipitator

Of the most commonly used particulate collection, electrostatic precipitators (ESP) are one of the more frequently used. They can handle large gas volumes with a wide range of inlet temperatures, pressures, dust volumes, and acid gas conditions. They can collect a wide range of particle sizes, and they can collect particles both in dry and wet states. For many industries, the collection efficiency can go as high as 99%. ESPs aren't always the appropriate collection device.

1.4 Theory of Precipitation

Every particle either has or can be given a charge—positive or negative. Let us assume we impart some negative charge to all the particles in a gas stream. Then we set up a grounded plate having a positive charge. Now the negatively charged particles would migrate towards the grounded collection plate and will be captured. The particles would quickly get collected on the plate, creating a layer of dust particles. The dust layer would accumulate until it is removed, which can be done either by rapping the plate or by spraying it with a liquid.

Charging, collecting, and removing—that's the basic working principle of an ESP (electrostatic precipitator).

1.4.1 Charging

A general electrostatic precipitator as shown in Figure 1.1 has thin wires known as discharge electrodes, which are evenly spaced between large plates called collection electrodes, which are grounded. A negative, high-voltage, pulsating, direct current is applied to these discharge electrodes thus creating a negative electric field.

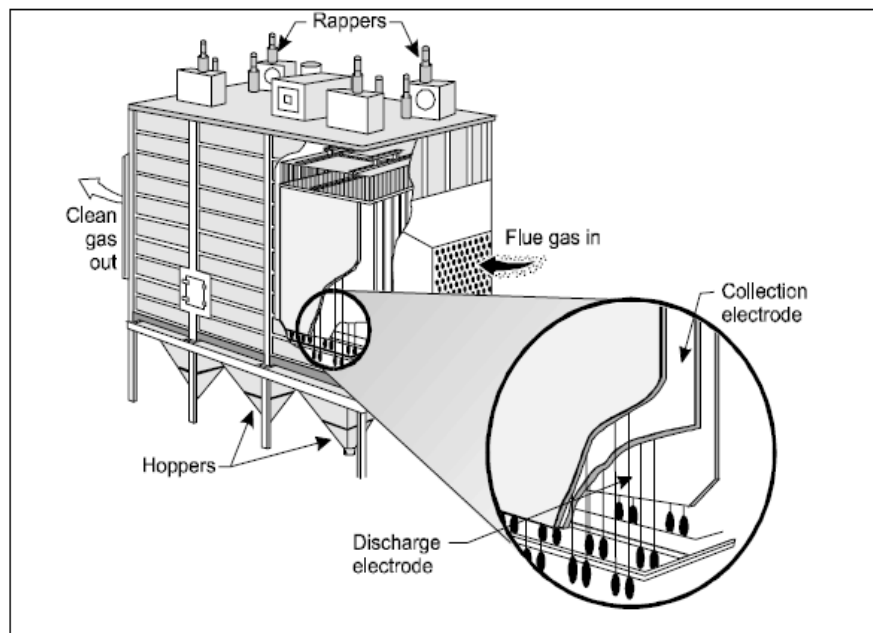


Figure 1.1: Typical dry electrostatic precipitator

This field can be divided into three regions as shown in Figure 1.2. The field is strongest right next to the discharge electrode, weaker in the areas between the discharge and collection electrodes called the inter-electrode region, and weakest near the collection electrode. The particle charging process begins in the region around the discharge electrode.

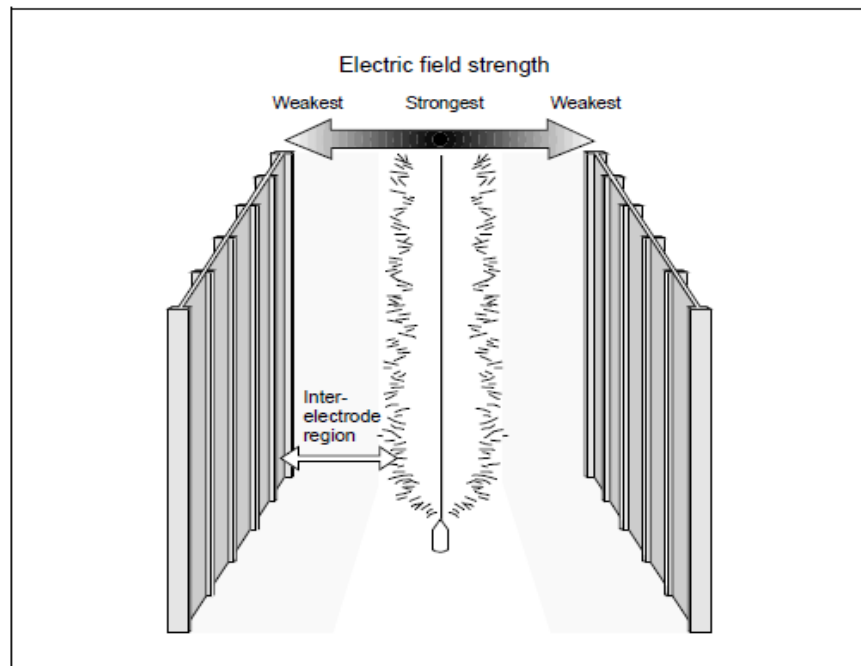


Figure 1.2: ESP electric field

1.4.1.1 Corona Discharge: Free Electron Generation

Several things happen very rapidly in the small area around the discharge electrode. The applied voltage is increased until it produces a corona discharge. This corona discharge can be seen as a luminous blue glow around the discharge electrode. The free electrons created by this phenomenon are rapidly fleeing the negative electric field, which repulses them. Thus they move at a high speed away from the discharge electrode. This acceleration causes them to crash into the gas molecules, bumping off electrons in the molecules. As a result of losing an electron, the gas molecule become positively charged resulting in positive ions (Figure 1.3).

All this activity occurs very close to the discharge electrode. This process continues, creating more and more free electrons and more positive ions. Thus, the first thing that happens is that the gas molecules are ionized, and electrons are liberated.

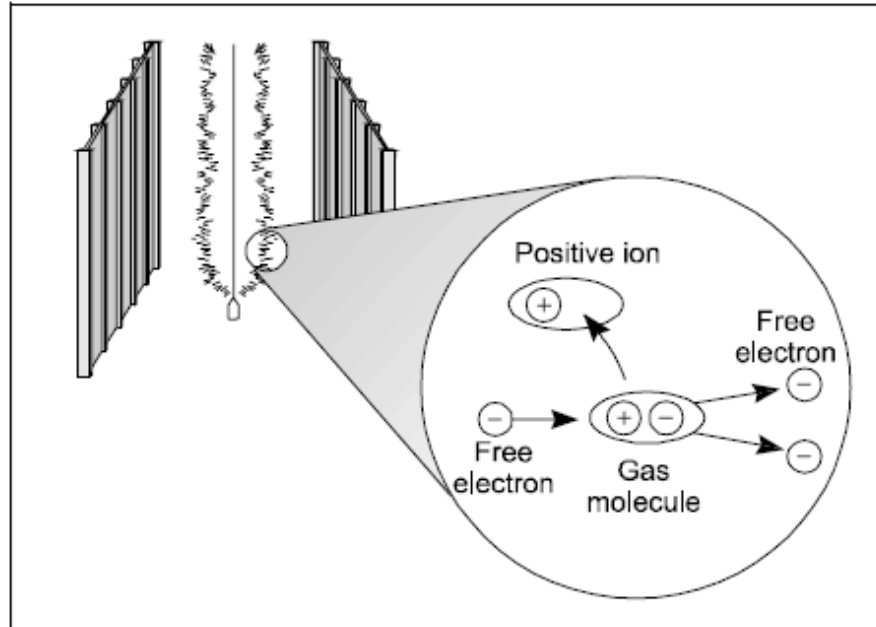


Figure 1.3: Corona generation

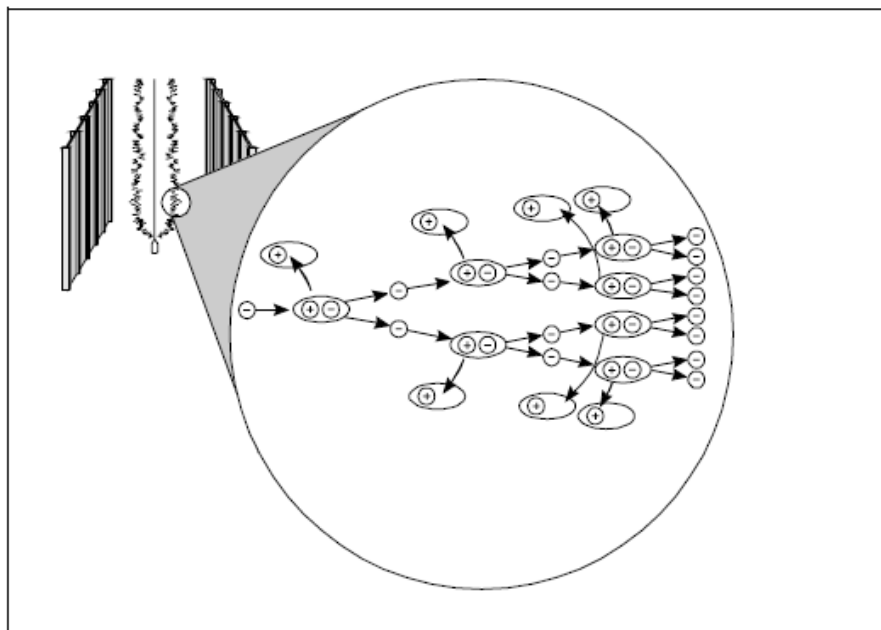


Figure 1.4: Avalanche multiplication of gas molecules

The electrons bump into gas molecules and create additional ionized molecules. This electron generation activity is known as avalanche multiplication as shown in Figure 1.4. The positive ions thus created, on the other hand, are drawn back towards the negative discharge electrode. The molecules are much bigger in size as compared to tiny electrons and move slowly, but they do pick up speed. In fact, many of them collide directly into the metal discharge electrode or the gas space around the wire causing additional electrons to be knocked off. This is known as secondary emission. After this we still have positive ions and a large amount of free electrons.

1.4.1.2 Ionization of Gas Molecules

When the electrons leave the strong electrical field area around the discharge electrode, they start to slow down. Now in the inter-electrode region, they are still repulsed by the discharge electrode but to a lesser extent. There are also gas molecules in the inter-electrode region, but instead of colliding with them, the electrons bump up to them and are captured (Figure 1.5).

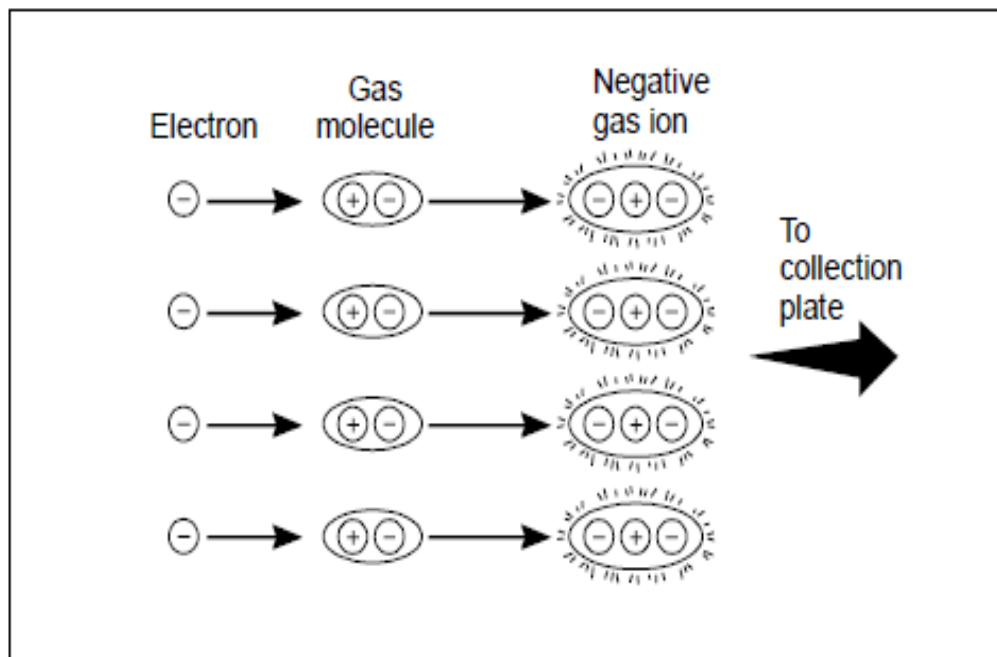


Figure 1.5: Negative gas ions formed in the inter-electrode region

This imparts a negative charge to the gas molecules resulting in negative gas ions. Now since the ions are negative, they too want to move in the direction opposite the strong negative field. The ions near the discharge electrode are positive and thus remain in that area. The ions in the middle area are negative and move away towards the collection electrode.

1.4.1.3 Charging of Particles

These negative gas ions play a key role in capturing dust particles. Before the dust particles can be captured, they must first acquire a negative charge. The particles are travelling along in the gas stream and encounter negative ions moving across their path. The gas ions stick to the particles, imparting a negative charge to them. At first the charge is fairly insignificant as most particles are huge compared to a gas molecule. But many gas ions can fit on a particle, and they do. Small particles (less than 1 μm diameter) can absorb “tens” of ions. Large particles (greater than 10 μm) can absorb "tens of thousands" of ions.

Eventually, there are so many ions stuck to the particles, the particles emit their own negative electrical field. When this happens, the negative field around the particle repulses the negative gas ions and no additional ions are acquired. This is called the saturation charge. Now the negatively-charged particles are feeling the inescapable pull of electrostatic attraction. Bigger particles have a higher saturation charge (more molecules fit) and consequently are pulled more strongly to the collection plate. In other words, they move faster than smaller particles. Regardless of size, the particles encounter the plate and stick, because of adhesive and cohesive forces.

As shown in Figure 1.6, the gas molecules around the discharge electrode are positively ionized. Free electrons are racing as fast as they can away from the strong negative field area around the discharge electrode. The electrons are captured by gas molecules in the inter-electrode area and impart a negative charge to them. Negative gas ions meet particles and are captured.

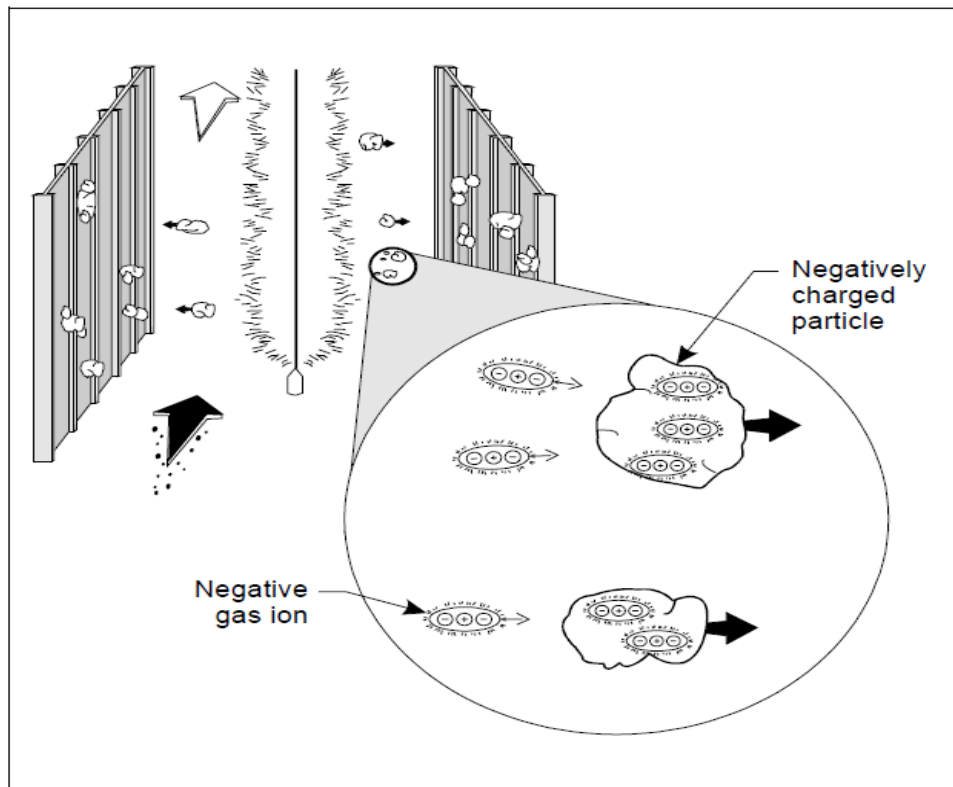


Figure 1.6: Particle charging

The net result is negatively charged particles that are repulsed by the negative electric field around the discharge electrode and are strongly attracted to the collection plate. They travel toward the grounded collection plate, bump into it, and stay there. More and more particles accumulate, creating a dust layer. This dust layer builds until it is somehow removed.

1.4.1.4 Particle Charging Mechanisms

The dust particles are charged by negative gas ions moving toward the collection plate by either of the two mechanisms: field charging or diffusion charging. In field charging, particles capture negatively charged gas ions as the ions move toward the grounded collection plate. Diffusion charging depends on the random motion of the gas ions to charge the particles.

In field charging (Figure 1.7), as particles enter the electric field, they cause the field to dislocate. Negative gas ions travelling along the electric field lines collide with the suspended particles and impart a charge to the particles. The ions will continue to bombard a particle until the charge on that particle is strong enough to divert the electric lines away. This prevents new ions to collide with the charged dust particle. When a particle no longer receives charge, it is said to be saturated. These saturated charged particles then migrate to the collection electrode and get collected.

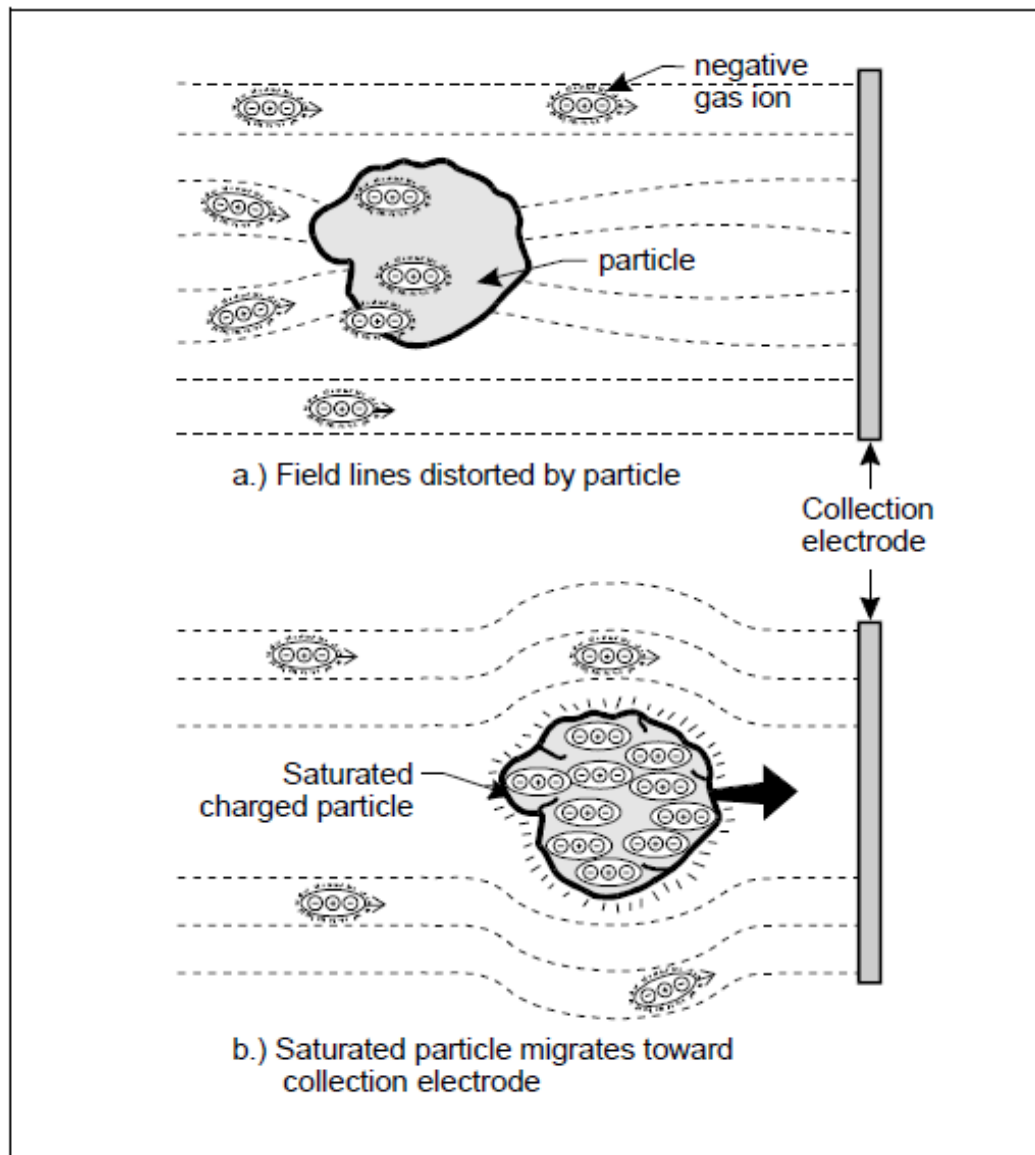


Figure 1.7: Field charging

Diffusion charging is associated with the random Brownian motion of the negatively charged gas ions. This random motion is related to the velocity of the gas ions due to thermal effects: the higher the temperature more is the movement. Negative gas ions because of their random thermal motion collide and impart a charge on the particles. Since the particles are very small, they do not cause the electric field to be dislocated. Thus, diffusion charging is the only mechanism through which these very small particles become charged. The charged particles migrate towards the collection electrode.

Each of these two charging mechanisms occurs, but one of them dominates depending upon the particle size. Field charging dominates for the particles with diameter greater than 1.0 μm while diffusion charging dominates for particles with a diameter less than 0.1 μm . A combination of these two charging mechanisms occurs for particles ranging between 0.2 and 1.0 μm in diameter.

A third type of charging mechanism, in which fast-moving free electrons that have not yet combined with the gas ions hit the particle and impart charge. This type of charging is known as electron charging and is very little responsible for particle charging.

1.4.2 Electric Field Strength

In the inter-electrode region, negative gas ions migrate towards the collection electrodes which are grounded. A stable concentration of negative gas ions is formed in the inter-electrode region because of the high electric field applied to the ESP known as space charge. Increasing the applied voltage to the discharge electrode increases the field strength and ion formation until sparkover occurs. Internal sparking between the discharge and collection electrodes is known as sparkover. In this there is a sudden rush of localized electric current between the two electrodes through the gas layer. Sparking causes an immediate short-term collapse of the electric field (Figure 1.8).

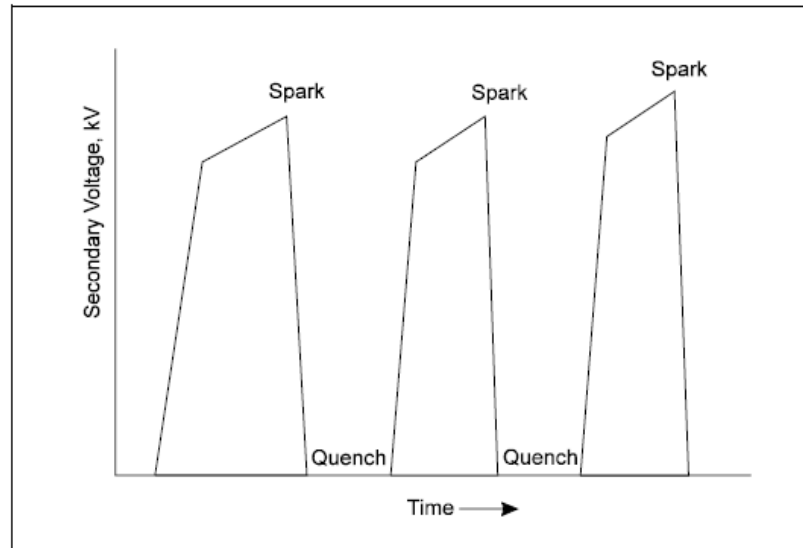


Figure 1.8: Spark generation profile

For optimum efficiency, the electric field strength should be as high as possible. Thus ESPs should be operated at voltages high enough to cause some sparking, but the collapse of the electric field should not occur too frequently.

1.4.3 Particle Collection

When a charged particle reaches the grounded collection electrode, the charge on the particle is only partially discharged. Then the charge is slowly leaked through the grounded collection plate. Some portion of the charge is retained which contributes to the inter-molecular adhesive and cohesive forces that holds the particles onto the plates (Figure 1.9). Adhesive forces cause the particles to physically hold on to each other because of their dissimilar surfaces. Newly arrived particles are attracted and held to each other molecularly by cohesive forces. The dust layer is allowed to build up on the plate to a desired thickness. After this the next step of particle removal cycle is initiated.

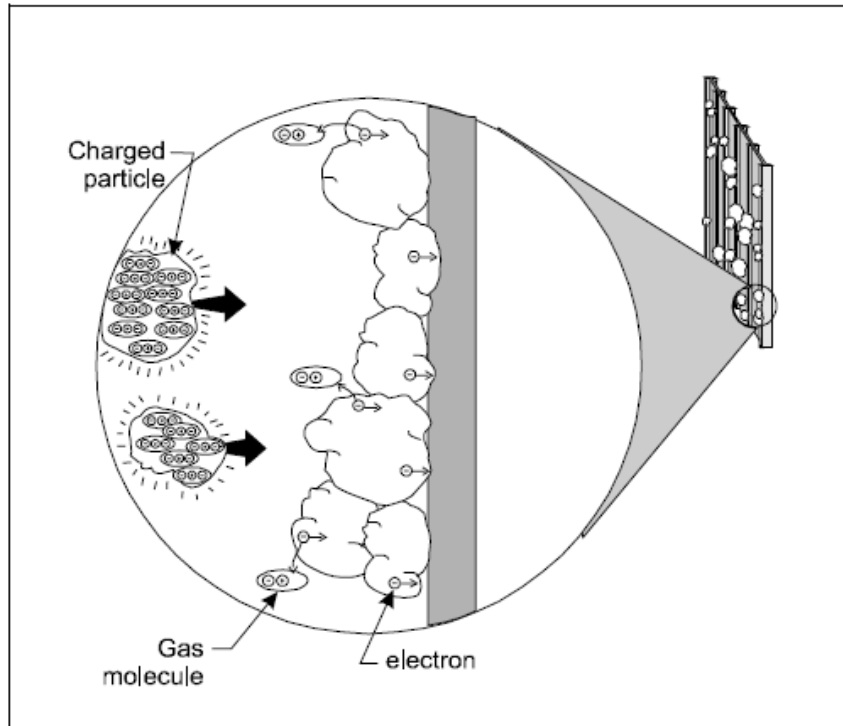


Figure 1.9: Particle collection at collection electrode

1.4.4 Particle Removal

Dust that has accumulated to a certain thickness on the collection electrode is removed by any one of the two processes, depending upon the type of collection electrode. Collection electrodes in precipitators can be either plates or tubes. Tubes are usually cleaned using water sprays, while plates can be cleaned either by using water sprays or through a process known as rapping.

Rapping is a process whereby deposited, dry particles are removed from the collection plates by sending mechanical impulses or vibrations to the collector plates. Plates are rapped periodically while maintaining the continuous flue-gas cleaning process. In other words, the plates are rapped while the ESP is on-line that is the gas flow continues through the precipitator and the applied voltage remains constant. Plates are rapped when the accumulated dust layer is thick (0.08 to 1.27 cm or 0.03 to 0.5 in.). This allows the dust layer to fall off the plates in the form of aggregate sheets and helps eliminate dust re-entrainment.

Most precipitators have adjustable rappers so that the rapping intensity and frequency can be changed according to the requirement that is dust concentration in the flue gas. Installations where the dust concentration is heavy require more rapping frequently. Dislodged dust falls from the plates into the hopper.

The hopper is a single collection bin with sides sloping downwards to allow the dislodged dust to flow freely from the top of the hopper to the discharge opening. Dust should be removed as soon as possible to avoid blocking of hopper. Most hoppers are emptied using some type of discharge device and then transported by a conveyor. In a precipitator, liquid sprays are used to remove accumulated dust. The sludge collects at the bottom of the vessel. The sludge is then sent to settling ponds or lined landfills for proper ultimate disposal. Spraying is done intermittently when the ESP is on-line to remove the collected particles. Generally water is used as the spraying liquid though other liquids can be used if absorption of gaseous pollutants is also being accomplished.

1.5 Steps for Working of ESP

Step for the working of ESP as charging, collecting, and removing:

- Gas molecules around the discharge electrode are positively ionized.
- Free electrons move away from the strong negative field area around the discharge electrode.
- The electrons are then captured by the gas molecules in the inter-electrode area and impart a negative charge to them.
- Negative gas ions meet particles and are captured.
- Then the negatively charged dust particles that are repulsed by the negative electric field around the discharge electrode are strongly attracted towards the collection plate.
- The dust particles travel towards bump into the collection plate and stay there.
- More and more particles get accumulated, creating a dust layer.
- This dust layer builds up until is removed by water spray or rapping.

1.6 Types of Electrostatic Precipitators

ESPs can be classified or grouped, according to a number of distinguishing features in their design. These features include the following:

- Based on structural design, operation of the discharge electrodes (rigid-frame, wires or plate) and collection electrodes (tubular or plate).
- Based on the method of charging of particles (single-stage or two-stage).
- Based on temperature of operation of ESP (cold-side or hot-side).
- Based on the method of particle removal from collection surfaces (wet or dry).

These categories are not mutually exclusive. For example, it can be a rigid-frame, single-stage, cold-side, plate-type ESP [2].

1.7 Electrostatic Scrubber

1.7.1 Introduction

Apparatus of many forms have been provided for the purpose of wet scrubbing a gas stream to remove the particulate material. Particles in a gas stream which measure between 1 and 3 micron in size, and those particles which are submicron in size tend to remain entrained in the gas stream. To collect particles of such small size with high efficiency electrostatic charging of the particles is done. Thus electrostatic charging of the droplets and particles to opposite polarity can substantially increase the particle collection efficiency of spray scrubbers, but more study is needed to obtain additional knowledge concerning this particle collection phenomenon.

1.7.2 Basic Working Principle

The cleansing of industrial exhaust gases using wet electrostatic precipitator technique is already studied. From this the electrostatic scrubber system was developed. Here electrostatic scrubber uses fine water spray droplets or cascading sheets of water in place of the conventional solid collector plates of an electrostatic precipitator.

The interaction of a finely atomized water spray uniformly charged to one polarity, with an oppositely charged aerosol, creates a combined spray scrubber and collector apparatus wherein charged particles are physically captured by the water droplets or cascading sheets of water enhanced by the attraction of the charged particles towards the oppositely charged spray droplets or sheet of water. These collector droplets, after the deposition of the dust particles, are removed from the apparatus and simultaneously fresh droplets enter the system. While along with this the polluted air enters the system, dust gets collected by the collector and clean air leaves the system. A schematic diagram of an electrostatic scrubber is shown in Figure 1.10.

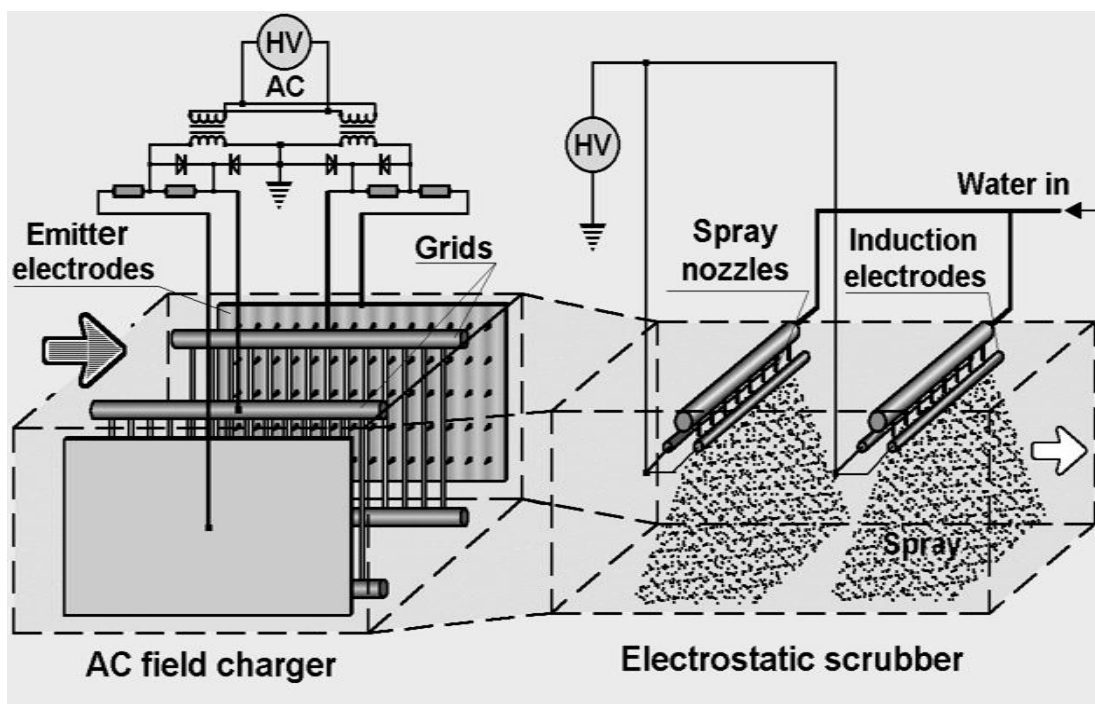


Figure 1.10: Schematic diagram of electrostatic scrubber

Following Coulomb's Law, the small particles are attracted towards and captured by the water droplets or sheet. The contact between the liquid spray and the aerosol containing gas stream is generally carried out in a large open container. Simultaneous measurements of the aerosol size distribution and mass concentration at the inlet and outlet of the electrostatic droplet spray scrubber showed that the overall particle collection efficiency increases considerably at uncharged conditions to charged conditions.

1.7.3 Difference between Electrostatic Scrubber and ESP

The method and apparatus of this are to be distinguished from electrostatic precipitators. In this respect, conventional electrostatic precipitators operate on the principle of first charging in an ionizing section and then passing the particles through an imposed electrostatic field wherein Coulomb forces act to drift the particle to a collecting surface.

While in electrostatic scrubber the ionized dust particle gets collected on the neutral or oppositely charged collector droplet instead of fixed collecting surface. The collector droplet may be a charged water droplet in this case. This droplet may be sprayed through a nozzle which collects the dust particles and flows out. Thus in this case there are no collector plates to be cleaned. Thus there is no wear and tear of the collector plates, thus reducing the overall size of the apparatus. Also the collection efficiency is high for submicron sized particles [3].

1.7.4 Advantages and Disadvantages

The advantages of the electrostatic scrubbers are as follows:

- Low investment costs
- Low power consumption (similar to electrostatic precipitators)
- Low water consumption (lower than in inertial scrubbers)
- Low wear and tear
- Low sensitivity to physical and chemical particle characteristics
- High collection efficiency in sub-micrometer range

1.7.5 Particle Deposition Mechanisms

The following mechanisms of particle deposition on a collector (a droplet) can be distinguished:

- Coulomb and image electrostatic forces and repulsive action of the space charge of equally charged dust particles cloud

- Polarisation forces between the particles placed in an external electric field
- Vortices downstream of the collector, occurring for high Reynolds numbers
- Brownian motion
- Thermophoresis
- Inertial impact
- Interception
- Gravitational sedimentation [3]

1.7.6 Some Important Features

According to the construction and features of the scrubber, it is important to model the system to study its working and efficiency. Thus the following features should be remembered before modelling of the electrostatic scrubber system is started.

- Scrubbing apparatus may take any number of a variety of forms comprised of features such as surface means, gas flow rate, liquid flow rate, droplet size, ionization type, force of attraction etc. The apparatus can be designed for various air velocities, it only being necessary that the particles have adequate residence time in the ionizer zone in order to be adequately charged. The scrubbing liquid is quite frequently water, however any suitable scrubbing liquid may also be used for this purpose.
- In any event, the gas stream is caused to flow at a low velocity relative to the neutral surfaces means and charged particles therein either impinge against the neutral surface means or are carried by the gas stream in close proximity thereto so that the force of attraction between the charged particles and neutral surface means will overcome the velocity of the particles and drag force of the gas stream thereon, thus to remove the particles from the gas stream by attraction to the neutral surfaces. The force of attraction between the charged particles and neutral packing elements and scrubbing liquid will cause the particles to be attracted to the scrubbing liquid or packing elements and be removed from the gas stream.

Normally, a negative charge is imparted to the particles in the gas stream for best corona discharge, but the charge can be positive. Further, alternate positive and negative charges in a gas stream such as by employing alternating current to energize the ionizer means. The nature of the particles to be removed from the gas stream will in part determine the polarity which provides for the best results to be achieved [4].

- The increase in droplets in turn increases the probability of charged particles passing sufficiently close at the same point during the travel through the apparatus for the force of attraction to be effective to remove the particles from the gas stream.
- The problem of calculating the effects of the electric field space charge is complex because the electric field strength and direction are dependent upon the location in the scrubber chamber and upon the droplet and aerosol charge and concentration distribution. However, in general it appears that the space charge will reduce the scrubber overall particle collection efficiency by two mechanisms: reduction of the single droplet particle collection efficiency by modifying the particle trajectory near the droplet, and by reduction of the droplet concentration in the scrubber as the charged droplets will be repelled by their like charges and migrate toward the scrubber chamber walls. Also, the theoretical model assumes that all particles that touch the droplet surface are collected. However, this does not probably occur [5].

CHAPTER 2

CONCEPT REVIEW

The thesis work made use some basic physics laws and mathematical concepts. A review of the basic idea for those is presented here.

2.1 Coulomb's Law

Coulomb's law, or Coulomb's inverse square law, is a law of physics which describes the electrostatic interaction between two electrically charged particles.

It states that: "The magnitude of the Electrostatics force of interaction between two point charges is directly proportional to the scalar multiplication of the magnitudes of charges and inversely proportional to the square of the distances between them."

The scalar form of Coulomb's law can be expressed by the magnitude and sign of the electrostatic force between the two idealized point charges, small in size compared to their separation. Let force (F) acting simultaneously on point charges (q_1) and (q_2), is given by:

$$F = k_e \frac{q_1 q_2}{r^2}$$

Where

r is the separation distance between two charges and

k_e is the proportionality constant.

A positive force implies that it is a repulsive force, while a negative force implies it is attractive in nature. The proportionality constant k_e , also known as the Coulomb constant is related to defined properties of space and can be calculated based upon the knowledge of empirical measurements of the speed of light [6]:

$$k_e = \frac{1}{4\pi\epsilon_0}$$

Vector form:

In order to obtain both the magnitude and the direction of the force on a charge, q_1 at position r_1 , experiencing a field due to the presence of another charge, q_2 at position r_2 , the full vector form of Coulomb's law is given by:

$$\mathbf{F} = \frac{1}{4\pi\epsilon_0} \frac{q_1 q_2 (\mathbf{r}_1 - \mathbf{r}_2)}{|\mathbf{r}_1 - \mathbf{r}_2|^3} = \frac{1}{4\pi\epsilon_0} \frac{q_1 q_2}{r^2} \hat{\mathbf{r}}_{21}$$

This is simply the scalar definition of Coulomb's law with the direction given by the unit vector $\hat{\mathbf{r}}_{21}$, parallel with the line from charge q_2 to charge q_1 .

If both the charges have the same sign (like charges) then the product $q_1 q_2$ is positive and the direction of the force on q_1 is represented by $\hat{\mathbf{r}}_{21}$; then the charges repel each other. If the charges have opposite signs then the product $q_1 q_2$ is negative and the direction of the force on q_1 is given by $-\hat{\mathbf{r}}_{21}$; then the charges attract each other [7].

2.2 Stoke's Law (Drag on a Particle)

The drag force is exerted on a particle as it moves in any fluid. This drag force is always present unless the particle is moving in a vacuum. To calculate the drag force exerted by the fluid on a particle moving in it we have to solve the equations of fluid motion to determine the velocity and pressure fields around the particle. The solution of the equations for the velocity and pressure distribution around a sphere in creeping flow was first obtained by Stokes. The assumptions lead to obtain that solution are: (1) an infinite medium, (2) a rigid sphere, and (3) no slip at the surface of the sphere. The main objective is to calculate the net force exerted by the fluid on the sphere in the direction of flow.

The total drag force exerted by the fluid on the sphere is:

$$\mathbf{F}_{\text{drag}} = \mathbf{F}_n + \mathbf{F}_t = 6\pi\mu R_p \mathbf{u}_\infty$$

Which is known as Stoke's law.

If we include gravity, the total force on the sphere is the sum of the drag force and the buoyant force. When the direction of flow and the direction of gravity coincide, the buoyant force to should be added to the drag force which is the force equal to the weight of the fluid displaced by the sphere,

$$F_{\text{buoyant}} = \frac{4}{3} \pi R_p^3 \rho g$$

To account for the drag force in terms of an empirical drag coefficient C_D as:

$$F_{\text{drag}} = C_D A_p \rho \frac{u_\infty^2}{2}$$

where A_p is the projected area of the body normal to the flow. Thus, for a spherical particle of diameter D_p ,

$$F_{\text{drag}} = \frac{\pi}{8} C_D \rho D_p^2 u_\infty^2$$

where the following correlations are available for the drag coefficient as a function of Reynolds number [8]:

$$C_D = \begin{cases} \frac{24}{Re}, & Re < 0.1 \\ \frac{24}{Re} \left(1 + \frac{3}{16} Re + \frac{9}{160} Re^2 \ln 2Re \right), & 0.1 < Re < 2 \\ \frac{24}{Re} (1 + 0.15 Re^{0.687}), & 2 < Re < 500 \\ 0.44, & 500 < Re < 2 \times 10^5 \end{cases}$$

2.3 Thermophoresis Force

Thermophoresis is the migration of a particle away from the higher-temperature region towards the lower-temperature region of the gas in which it is suspended. The motion is caused due to the greater force imparted by the higher energy molecules on the hot side of the particle than by those on the cold side. This phenomenon is responsible for soiling of the walls in the vicinity of hot pipes. In the absence of all the other forces, the thermophoretic force will be balanced only by the drag force, thus leading to a steady thermophoretic velocity [9].

2.4 Diffusiophoresis Force

Diffusiophoresis occurs in the presence of gradient of vapour molecules that are either lighter or heavier as compared to the surrounding gas molecules [10]. For example, consider an evaporating surface over which a gradient of water vapour concentration exists. Water molecules are less massive as compared to the air molecules, so decrease in water vapour concentration with the distance above the evaporating surface will lead to a resultant downward force on aerosol particles, that is, the result of the downward flux of air molecules needs to balance the upward flux of water molecules [10].

2.5 Image Force

Suppose a positively charged particle is moved to a location at a distance h above a grounded conductor, negative charge will be induced on the conductor (in order for it to remain at ground) and the negative charge will be concentrated at a position closest to the positive charge on the conductor. If the conductor is an infinite plane (that is its edges are at distances $\gg h$) then the field generated by the charge arrangement induced on the plane is exactly the same as the field due to a mirror image negative charge located a distance h below the plane. This shows that the charged particle will be attracted towards the plane with a force that varies as the inverse of the square of h [11].

If the grounded conductor is spherical, the effects of induced charge can be represented with an image charge, although with a little more complexity. For more generally shaped grounded conductors we use the expression image force somewhat loosely to describe the attraction of a charged body to the conductor. The image forces are unavoidable and at micro levels image force increases with decrease in distance more quickly than any other controllable force. At small distances the strong image forces act to make the distances smaller and thereby create a positive feedback loop which ends with surfaces sticking [10]. Although image force plays an important part, yet its value is not clearly defined thus it can be neglected for the time being from the present calculations.

2.6 Reynolds Number

Observations show that in any system involving fluid flow both for gas or liquid, two completely different types of flow can exist, that is laminar flow or turbulent flow. In laminar, viscous or streamline, the particles of fluid move in an orderly manner and retain the same relative positions in successive cross-sections. Turbulent flow is characterized by continuous small variations in the magnitude and direction of the velocity of the particles, which are accompanied, by corresponding small variations of pressure.

When the motion of a fluid particle in a given stream is disturbed, its inertia will tend to carry it in a new direction, but the viscous forces acting on it due to surrounding fluid will tend to make it conform to the motion of the rest of the stream. In viscous flow, the viscous forces are sufficient enough to eliminate the effects of any deviation, but in turbulent flow, they are deficient. The criterion, which determines whether the flow will be viscous or turbulent, is defined by the ratio of the internal force to the viscous force acting on a particle.

By dividing the characteristic inertia forces of the fluid flow to characteristic viscous forces of the same flow, it is found that the ratio is proportional to dimensionless value [13].

$$\text{Re} = \frac{\rho v l}{\mu}$$

where:

ρ is fluid density,

v is characteristic fluid velocity,

l is characteristic length of the fluid flow,

μ is dynamic viscosity of the fluid.

This dimensionless value Re is known as Reynolds number. The value of the Reynolds number at which the flow ceases to be laminar and becomes turbulent depends upon the flow geometry. However, usually the transition of flow from laminar to turbulent occurs in the range 1,000-10,000 for Reynolds number [14].

2.7 Navier-Stokes Equation

To obtain the velocity, pressure, and/or temperature for any fluid flow one has to solve the equations of motion of the fluid along with energy equation and equation of state of the fluid using appropriate boundary value conditions. Theoretically, for the equations of motion for both laminar and turbulent, Newtonian flows are given by Navier-Stokes equations.

However, in practice the solution of Navier-Stokes equations requires very small computational cell size since we need to simulate accurately. This leads to very large amount of computations. Moreover, this kind of precision normally is not required for the engineering systems where usually only time-averaged values of the flow are important. To avoid this, Navier-Stokes equations are directed to determine the time-averaged values of the velocities and pressure rather than instantaneous values of these parameters [15]. In general, the air flow is governed by the Navier–Stokes equation, which is a set of nonlinear partial differential equations with unknown components of the velocity vector and pressure.

For the purpose of simulation of aerosol particle deposition on the spherical collector the problem has been simplified by the introduction of 2 scalar variables, the stream function Ψ and vorticity ω . For finite and nonzero Reynolds numbers, the partial differential equations for Ψ and ω are mutually coupled and are needed to be solved simultaneously.

However, the problem is very often simplified by neglecting viscosity, that is assuming $Re = 0$ or $Re = \infty$. For calculating the nonviscous case (potential flow), a second-order partial differential equation is to be solved. These equations can be solved simultaneously, but iterative algorithms are used for simplicity and this seemed to be very effective. Assuming zero vorticity, equations can be solved for stream function. Then the stream function is substituted, and solved for ω . The process is continued until convergence is reached. The rate of convergence depends on the value of Re (Reynolds number). Only a few iterations are sufficient when Re is close to zero while a much higher number is required for large values Re .

The boundary conditions are to be formulated for all involved functions. They result from the assumption that initially the flow is undisturbed and uniform and both components of the velocity vector vanish on the droplet surface. Using these conditions, any iterative technique along with finite element method can be applied. Thus it was difficult to find a reliable and accurate solution to this problem.

2.8 Numerical Algorithm (Numerical analysis method)

Differential equations can be used to describe nearly all systems undergoing change. They are widespread not only in physics, engineering, economics, social science, but also in biology. Many researchers have studied the nature of these differential equations and have used these to describe many complicated systems quite precisely. However, many systems involving differential equations are so complex, or the systems that they describe are so large, that a purely mathematical analysis is either not possible or is not enough to explain the systems completely.

It is in these complex systems where computer simulations and numerical approximations come into focus. The techniques for solving these differential equations based on numerical approximations were designed long before programmable computers existed. People working on mechanical calculators to solve these equations could be easily seen. Since computers have increased in speed and decreased in cost, increasingly complex systems of differential equations can be solved easily on a common PC.

When solving differential equations numerically, it is generally seen that it is convenient to work with equations involving only first derivatives since the same program can be generalized to solve any problem. When constructing solutions to any differential equations it is always easier to recast the equations into a form that has no dimensions, i.e. the equations do not depend upon parameters that have units such as meters, seconds, etc. because rescaling the equations will always reduce the number of free parameters that can be varied. Thus this scaling means that we need to solve the system of equations only once, plot the solution in non-dimensional form and anyone can now use this to find dimensional solutions by multiplying the solution by a constant instead of solving the whole system of equations for each choice of parameters, thus solving needs to be done only once [16].

2.8.1 Principle

Most often, systems of differential equations cannot be solved analytically. Algorithms based on numerical methods are therefore are to be used. Numerical integration means to compute the variable say for example x , from an initial point x_0 (the initial condition), at each successive point x_1, x_2, x_3, \dots that satisfies the evolution equation:

$$\frac{dx}{dt} = f(t, x)$$

Thus an algorithm computes as precisely as possible x_{n+1} from x_n .

2.8.2 Euler's Method

The first basic method is Euler's algorithm can be explained. For example consider the following differential equation:

$$\frac{dx}{dt} = f(t, x) \quad (1)$$

The formula for the Euler method is:

$$x_{n+1} = x_n + \Delta t f(t_n, x_n) \quad (2)$$

In a given time step Δt (predefined by the user), the formula thus directly calculates the point x_{n+1} from the x_n by calculating the derivative at x_n . Euler's method is not recommended for practical use because it is not very accurate as compared to other methods that run using the equivalent step size. The imprecision comes from the fact that the derivative between t_n and $t_n + \Delta t$ changes while Euler formula relies only on the derivative at time t_n . Smaller the step size, smaller will be the error [17].

For better accuracy without requiring much extra work an alternative numerical method known as Backward Euler Method can be used. This method is as explained below:

Equation (2) from Euler's method can be written as:

$$f(t_n, x_n) \approx \frac{x_{n+1} - x_n}{\Delta t} \quad (3)$$

We thus compute x_{n+1} assuming that the derivative at point (t_{n+1}, x_{n+1}) is the same as at point (t_n, x_n) :

$$f(t_{n+1}, x_{n+1}) \approx \frac{x_{n+1} - x_n}{\Delta t} \quad (4)$$

We then find that :

$$x_{n+1} = x_n + \Delta t f(t_{n+1}, x_{n+1}) \quad (5)$$

Thus we can find x_{n+1} from x by solving the algebraic equation (5). This is the backward Euler method. The backward Euler method is said to be implicit because we do not have an explicit expression for x_{n+1} . It costs CPU time to solve this equation and this cost must be taken into consideration while selecting the method to use. The advantages of implicit methods is that they are usually more stable for solving a stiff equation, that is a larger step size Δt can be used [18].

Further improvement of these methods leads us to Runge & Kutta algorithms.

2.8.3 Second-Order Runge- Kutta Method

Another estimation of the slope is the derivative at the mid-point between t and $t+\Delta t$. Initially consider the step like the one defined by the Euler formula (2). Then we can use the value of both t and x at that mid-point to compute the real step across the whole interval. It uses a fixed step size h .

The equations are then:

$$s_1 = f(t_n, y_n),$$

$$s_2 = f\left(t_n + \frac{h}{2}, y_n + \frac{h}{2} s_1\right),$$

$$y_{n+1} = y_n + h s_2$$

$$t_{n+1} = t_n + h$$

This method is called the second-order Runge & Kutta algorithm or the mid-point method.

2.8.4 Fourth-Order Runge & Kutta Method

More often used is the classical four-order Runge & Kutta algorithm. Instead of using the midpoint to estimate the derivative, the shooting across the entire interval the Runge-Kutta method takes four steps, shooting across one quarter of the interval, estimating the derivative, and then shooting to the midpoint, and so on.

$$s_1 = f(t_n, y_n),$$

$$s_2 = f\left(t_n + \frac{h}{2}, y_n + \frac{h}{2} s_1\right),$$

$$s_3 = f\left(t_n + \frac{h}{2}, y_n + \frac{h}{2} s_2\right),$$

$$s_4 = f(t_n + h, y_n + h s_3),$$

$$y_{n+1} = y_n + \frac{h}{6} (s_1 + 2s_2 + 2s_3 + s_4),$$

$$t_{n+1} = t_n + h$$

Here each time step requires 4 evaluations of the derivatives, i.e. the function f . Thus, the next value (y_{n+1}) can be determined by the present value (y_n) plus the product of the size of the interval (h) and an estimated slope. The slope is a weighted average of slopes:

- s_1 is the slope at the beginning of the interval;
- s_2 is the slope at the midpoint of the interval, using slope s_1 to determine the value of y at the point $t_n + h/2$ using Euler's method;
- s_3 is again the slope at the midpoint, but now using the slope s_2 to determine the y -value;
- s_4 is the slope at the end of the interval, with its y value determined using s_3 .

- In averaging the four slopes, higher weight is given to the slopes at the midpoint:

$$\text{slope} = \frac{1}{6} (s_1 + 2s_2 + 2s_3 + s_4)$$

As with the previous methods the error depends on the step size. Small step size leads to a better precision, but require larger CPU time. In this the adaptive step size method allows changing the step size during the integration [19].

2.9 MATLAB Functions

There are many mathematical softwares that have built-in function to perform numerical integration of ODE. MATLAB has several ODE solvers and provides some recommendations in Table 2.1:

Table 2.1: MATLAB command recommendations.

| Method | Problem type | Accuracy | When to use |
|--------|--------------|------------|---|
| Ode45 | Nonstiff | Medium | Most of the time, should be the first solver to try. |
| Ode23 | Nonstiff | Low | For problems with crude error tolerances or for solving moderately stiff problems. |
| Ode113 | Nonstiff | Low/high | For problems with stringent error tolerances or for solving moderately stiff problems. |
| Ode15s | Stiff | Low/medium | If ode45 is slow because the problem is stiff. |
| Ode23s | Stiff | Low | If using crude error tolerances to solve stiff systems and the mass matrix is constant. |

MATLAB has a solver that is called ODE45. The ODE45 command uses the Runge-Kutta algorithm, MATLAB uses adaptive time stepping [20].

CHAPTER 3

LITERATURE REVIEW

3.1 Wet Electroscrubbers for State of the Art Gas Cleaning

In 2006, A. Jaworek *et al.* presented a critical review paper where they said that: The principles of electrostatics were discovered by Coulomb (1785) and first successfully applied to the control of particulate air pollutant emissions by Cottrell (1908) whose research results gave rise to the large-scale utilization of dry electrostatic precipitators as industrial gas cleaning devices. After many researches in the mid 1950's, wet electrostatic precipitators were developed which used water to wash the particle collection electrodes. Thus, these wet electrostatic precipitators still have the same general configuration as dry precipitators with an additional feature of water-cleaned plates. After this electrostatic space charged scrubbers involving water droplets and aerosol particles with some charge was suggested by Hanson and Wilke (1969) [22]. In this the dust was collected onto the scrubber walls when droplet and dust were charged to same polarity and onto the collector droplet when they were charged with opposite polarity.

3.2 Collection of Aerosol Particles by Electrostatic Droplet Spray Scrubber

In 1974 M. Pilat *et al.* showed experimentally using a double chamber electrostatic droplet spray scrubber, that the collection of small aerosol particles (0.05 to 5 μ diameter range) by water droplets in spray scrubbers can be increased substantially by electrostatic charging of the droplets and particles to opposite polarity. The collection efficiency for 0.3 μ particles increased from 68.8% to 93.6% when the change was studied from uncharged to charge collector for rest of the conditions fixed [23].

3.3 Capture of Aerosol Particles by Spherical Collectors: Electrostatic, Inertial, Interception, and Viscous Effects

In 1974, H. George *et al.* presented a mathematical model for the collection of aerosol particles smaller than 10 μ m considering inertial, viscous, gravity, and electrostatic forces and interception phenomena. They also showed that collection efficiency could be improved by the presence of electrostatic charges on particles. The mathematical model was solved using Runge-Kutta type integration algorithm to calculate the trajectory of the particles. But the results were left for experimental verification [24].

3.4 Collection of Inertialess Particles on Spheres with Electrical Forces

In 1976, K. Nielsen *et al.* predicted particle trajectories and target efficiencies for the collection of fine particles on a single spherical collector in a gaseous flow field under the influence of electrical forces and in the absence of particle inertia. The electrical forces considered were Coulomb forces, electrical image forces, and external electric field forces. Analytical solutions showed that the collection efficiency of inertialess, point particles under the influence of coulomb and external electric field forces could be increased significantly. The results were extended to Oseen flow and to inclusion of gravitational forces [25].

3.5 Capture of Particles on Sphere by Inertial and electrical Forces

In 1976, K. Nielsen *et al.* in another paper first formulated the equations of particle motion for the combined influences of particle inertia and electrical forces. The electrical forces considered were coulomb forces, electrical image forces, and external electric field forces. Potential flow and Stokes flow were used to model the gas flow around the collector. From this the target efficiencies for the collection of fine particles by a single spherical collector in a gaseous flow field were calculated.

The calculations indicate that under favourable conditions all of the electrical forces considered significantly enhance particle collection over that obtained by inertial impaction alone. In general, the introduction of particle inertia to a given electrical force produced a greater change in the collection efficiency for potential flow as compared to that for Stokes flow. With weak electrical forces efficiency often passed through a minimum as K increased from zero [26].

3.6 Charged particle Collection by an Oppositely Charged Accelerating Droplet

In 1986, H. Wang *et al.* derived a theoretical model to predict the collision efficiency of an accelerating droplet under the combined effects of inertial impaction and electrostatic attraction for an accelerating collector as a function of downstream distance. The calculated efficiencies were reported as a function of the distance traversed by the droplet.

The numerical results of free stream collector with Reynolds number of range 50-800 were plotted. There was an increase in collection efficiency with increasing downstream distance. Curves corresponding to different Stokes numbers were plotted. The calculated results were approximated very well by a fifth-order polynomial. This model was verified by measuring the total particle mass collected by an accelerating droplet [27].

3.7 The Modelling of Electrostatic Forces in Small Electrostatic Actuators

In 1988, R. Price *et al.* presented briefly various electrostatic elements and interactions such as conductors, dielectrics, ferroelectrics, image forces, dielectrophoretic forces, etc. for the better understanding and modelling of electrostatic systems for various materials [28].

3.8 Collection of Aerosol Particles in Presence of Electrostatic Field

In 1995, H. Kraemer *et al.* gave a general theoretical solution and experimental verification for the deposition of aerosol particles from moving stream onto stationary spherical surfaces and an introductory study of the deposition on cylinders. Various types of forces were introduced and differential equations that describe the path of the particles were solved numerically using the ILLIAC digital computer. Collection efficiency was calculated and verified experimentally.

And finally two new types of dust collection equipment were proposed, electrified wet scrubber and an electrified filter mat. They showed experimentally that low relative velocities between the aerosol and collecting surfaces leads to increased collection efficiency [29].

3.9 Deposition of Aerosol Particles on a Charged Spherical Collector

In 1997, K. Adamaik *et al.* developed a numerical model for determining the trajectories of spherical aerosol particles in the vicinity of a charged spherical collector. The Coulomb, image Stokes and gravitational forces acting on the particle and the collector were considered in the equations of motion. The flow field was determined by numerical simulation of the Navier-Stokes equations using stream function and vorticity terms.

The graphs were plotted for few values of Coulomb and Reynolds numbers in xy plane, both for fixed value and zero image force. They showed that image forces are only effective for short distances. For small Reynolds and Stokes numbers the electrostatic forces are dominant that is for low relative velocities only, while with the increase in Stokes number the electrostatic effect diminishes [30].

3.10 Deposition efficiency of dust Particles on a Single, Falling and charged water Droplets

In 1998, K. Adamaik *et al.* in another paper presented a numerical algorithm for simulating the deposition process in wet scrubbing. They implemented a mathematical model in which the trajectories of particles and droplet were simultaneously traced by solving Newton equation, taking into account inertial, air drag, gravitational and electrostatic forces. The results of simulation showed that the process was controlled by a few parameters only: the Stokes, Coulomb, and Reynolds numbers. Image forces were assumed zero.

The collector falls down freely and its trajectory was also determined. Gravity modifies the vertical component and air drag entrains in the horizontal direction. Viscous laminar air flow was governed by Navier-Stokes equation using vorticity-stream function parameters. The finite element method and iterations in two-dimensional co-ordinates were used for solving the partial differential equations. The trajectories were traced using Runge-Kutta technique. They showed that for small Stokes number and zero Coulomb number air drag practically controls the particle movement and the deposition efficiency is minimal.

The deposition efficiency was calculated in terms of volume of space. They also showed that electric forces significantly improve deposition efficiency. For large Stokes number the particle inertia became the most crucial factor. The electric force in this case still slightly modified the trajectories, but did not affect the collection efficiency a lot. The Reynolds number in all cases was a secondary effect influencing the deposition [31].

3.11 3D Model for Trajectories of Airborne Particles near a Charged Spherical Collector

In 1998, A. Jaworek *et al.* presented a paper which defined numerical model for determining the trajectories of charged airborne particles in vicinity of much larger, oppositely charged spherical collector (a droplet) falling down freely.

Approximate equations of the flow field around the collector were described for a fixed collector. They used attractive Coulomb force to remove the particles which removed the short comings of the inertial scrubbers. The differential equations of the collector were solved simultaneously with the differential equations of the particle using fourth order Runge-Kutta technique. Image forces were neglected when compared to the large Coulomb force. Normalized form of the differential equations was used. The flow field was determined using the Navier-Stokes equation resulting in non-linear partial differential equations and used stream function and vorticity for approximation. These equations were solved using iterative methods using boundary values and Taylor's formula using further complex methods such as upwinding, which may be unstable if discretization was not sufficient. Furthermore the finite element method was used to solve the problem. The particle trajectories were simulated in 3-dimensionoal space and plotted only in $z=0$ plane.

From the equations of motion the limiting trajectories of the particles were determined. These trajectories allowed determining the precipitation space which measured the collection efficiency. The graphs were plotted for different values of Coulomb number, Stokes number and Reynolds number for constant collector diameter [32].

3.12 Submicron Charged Dust Particles Interception by charged Drops.

In 1998, A. Jaworek et al. in another paper presented the numerical algorithm for simulation of the trajectories of charged dust particles moving horizontally in vicinity of a freely falling, oppositely charged liquid space relative to the liquid droplet. The air drag, electrical and gravitational forces were considered. The trajectories were determined from the differential equations. The creeping air flow was determined using stream function. The solution for stream function was calculated using Oseen's linearized equation.

The limiting trajectories of the dust particles and the precipitation space varied with the value of Stokes number, which is mainly a function of the gas collector relative velocity, and Coulomb number, which depends principally on the charge of the collector and dust particle. In this collection efficiency was calculated using ratio of volume of the precipitation space to volume swept by collector. These results were numerically validated by the author. This showed that collection efficiency increased almost linearly with increase in the surface charge density. They also showed that collection efficiency could be improved using smaller water droplets. The deposition of dust particles on a collector due to the electrostatic forces was dominant only for small Stokes numbers [33].

3.13 Numerical Simulation of Scavenging of Small Particles by Charged Droplets.

In 2002, A. Jaworek *et al.* in another paper plotted the trajectories of fine aerosol particles in the vicinity of a freely falling charged collector droplet. The Coulomb, image, Stokes, inertial and gravitational forces acting upon the particle were taken into consideration in the equations of motion. The equations of the droplet motion were incorporated into the set of equations including Coulomb and image forces on the droplet due to particle charge.

The flow field in the vicinity of the droplet was determined by numerical solution of the Navier–Stokes equations. The equations of particle motion were solved in three dimensional (3-D) space by the Runge–Kutta method of the fourth order. The collection efficiency of the particles on the droplet was determined by searching the limiting trajectory within the entire space. The Navier–Stokes equations were solved in order to determine the flow field around the droplet using stream function and vorticity. The boundary conditions were formulated and FEM was used to solve these. The problem was studied for the droplet and particles charged to the same and opposite polarities. The model validated for particles larger than 1 μm . Results were compared with a simple trial-and-error method is used.

They showed that at long distances only Coulomb forces were dominant and drove the particles to the collector, while the image forces were significant if the particles were close to the droplet and only slightly enhanced the deposition process. Graphs were plotted for different collector diameters with both charged and uncharged droplets. Efficiency was calculated using ratio of volumes swept. The practical conclusion was that smaller droplets were more effective in the removal of fine particles due to lower terminal velocities of the droplets and stronger image forces. The specific water consumption was determined for the particles of various sizes. The volume of water necessary for cleaning the same space decreased with a decrease in the droplet diameter. Removal of smaller particles from gas required higher water consumption for the same collection efficiency [34].

CHAPTER 4

PROBLEM FORMULATION

One of the major causes of air pollution is the presence of particulate matter in the form of dust in amounts that may be harmful to human, plant or property. We know air pollution has adverse effects and can lead to serious problems. Natural events have been a direct cause of enormous air pollution but still the pollution caused by human activities is comparatively much greater. With the rapidly expanding industry, the concern over the control of man-made air pollutants is now clearly a necessity. Effective ways must be found to reduce and control air pollution.

Once the basic mechanism and their theory of control are mastered then we need to understand how to implement this information effectively in real situations. Several alternatives are available based on different mechanisms. Thus we need to optimize our solution according to the situation and need.

Many different types of control techniques that are using different type of forces or laws of operation can be used to achieve low dust emissions. Forces such as thermophoresis, diffusionphoresis, interception, centrifugal, condensation or electrostatic force or bio-filtration etc. can be used.

Many authors have studied different phenomena to design various types of systems. One of the methods which showed high efficiency and good results was the use to electrostatic force. The system designed using this force was named as electrostatic precipitator. To enhance its efficiency and overcome the advantages it was further embedded with features of scrubbers. Thus is known as electrostatic scrubber.

The electrostatic scrubber uses charged collector droplets to collect the dust particles of same or opposite polarity. In this Coulomb's force of attraction plays the major role for the deposition of dust on the collector.

To study the performance of a given electrostatic scrubber we need to calculate its dust collection efficiency, that is percentage of particles collected by the droplet. For this we have to study the behaviour of the particle as well as the collector in the charged conditions. Thus the behaviour of both can be studied by plotting the trajectories of both the dust particles and the collector simultaneously under a defined set of conditions.

Many researchers, in past, have traced the trajectories and studied the collection efficiency. For all the papers, one basic equation of motion was used to study the motion of dust particle. But along with this, few of them used stream function and calculated trajectories using numerical techniques such as finite element method, which makes it difficult to understand and calculate the path followed by the dust particles.

Moreover, in all the papers the information regarding how the numerical techniques are applied is eluding. Thus we here wish to get an alternate method of plotting these trajectories and thus calculating the dust collection efficiency in a simplified manner.

The trajectories can be plotted simply by calculating the co-ordinates of the dust particle and the collector droplet at each instant of time.

Thus our aim here is to plot the trajectories of the dust particle and to calculate the efficiency of the scrubber system.

CHAPTER 5

METHODOLOGY

The focus here is gas cleaning from fine dust particles by means of their deposition on the charged droplets. The collection of dust particles by the means of electrically charged droplets has been investigated numerically. The path traversed by the dust particle has been traced and collection efficiency of the scrubber is calculated.

5.1 Mathematical Model

The prediction of particle trajectories requires a detailed understanding of the forces acting on both the particle as well as on the collector. Thus the knowledge of various forces acting on the particle needs to be studied. When the particle and the droplet are charged to opposite polarities the dust gets collected on the collector. In case both the droplet and the particle are charged to the same polarity, the repulsive forces drive the particle to the scrubber walls where they are washed out [21].

5.2 Idealizing Assumptions

In order to solve the problem of particle deposition on a collector drop, many simplifications in the models are assumed here. The numerical algorithm traces simultaneously the mutual movement of two objects: a dust particle and a droplet.

The first assumption is that the complex set of interacting particles and droplet is reduced to a two-body system. That is the concentration of dust particles has been assumed to be small, therefore, the electric field of the space charge is much weaker than the field of the droplet. As a result, the electric force produced by other charged particles has been assumed to be insignificant and an interaction of either the particle or the collector with other objects is ignored. The second simplification is that both objects are assumed spherical and their shape is not distorted during the motion. This assumption implies that the equations of motion valid for idealized objects can be applied.

The third assumption is that the particle is much smaller than the droplet, and that the flow field in the vicinity of the droplet is not distorted by the particle.

The fourth assumption is that the drop does not evaporate, the water vapour does not condense on the particles, and the transfer of momentum and electric charge of particles to the collector droplet can be neglected. Wall effects, such as particle diffusion to the chamber walls are ignored and it is assumed that the particle and the collector are flowing in free space.

The fifth assumption is that the deposited dust particles do not change the droplet mass and charge. Practically, this affects the process, but it would require additional information about the dust concentration in the chamber and so it was also neglected [31].

We assume a single, spherical dust particle with radius R_p , charge Q_p and initial horizontal velocity u_0 , equal to the velocity of flowing gas. Its movement is affected by many forces such as the inertial, air drag, gravitational, Coulomb, and image, basset, thermophoretic and diffusiophoretic forces. Thus its path depending upon the affect these forces can be defined by numerical equations.

The droplet is also spherical with a given radius R_c and is electrically charged with a charge Q_c . It enters the scrubbing channel with some initial velocity v_0 , the vertical component. The droplet experiences forces in the channel. Therefore, it follows a complicated trajectory which is numerically traced [31].

5.3 Theoretical Background

5.3.1 Particle Trajectories

The problem of electro-scrubbing is usually considered as an interaction of fine particles and much larger spherical collectors. The trajectory of a particle of mass m_p is given by the following Newton vector differential equation [22]:

$$m_p \frac{d\vec{w}}{dt} = \vec{F}_A + \vec{F}_e + \vec{F}_B + \vec{F}_T + \vec{F}_D + \vec{F}_g \quad (1)$$

Where,

m_p is the particle mass,

w is the particle velocity,

\vec{F}_A is the aerodynamic drag,

\vec{F}_e is the electrical force,

\vec{F}_B is the Basset force,

\vec{F}_T is the thermophoresis force,

\vec{F}_D is the diffusiophoresis force,

\vec{F}_g represents the gravitational force.

The left hand side of equation 1 is the inertial force of the particle. The electrostatic force on the particle with image-charge effects included is as follows [22]:

$$F_e = -\frac{Q_p Q_c}{4\pi\epsilon_0 r^2} + \frac{R_p Q_c^2}{4\pi\epsilon_0 r^3} \frac{\epsilon_p - 1}{\epsilon_p + 2} \left(\frac{r^4}{(r^2 - R_p^2)^2} - 1 \right) + \frac{R_p Q_p^2}{4\pi\epsilon_0 r^3} \frac{\epsilon_c - 1}{\epsilon_c + 2} \left(\frac{r^4}{(r^2 - R_c^2)^2} - 1 \right) \quad (2)$$

where Q_p and Q_c are the charges on the particle and the droplet, respectively, R_p and R_c are the radii of the particle and the droplet, respectively, r is the distance between the particle and the droplet centres, ϵ_0 is the permittivity of the free space, and ϵ_p , ϵ_c are the relative permittivities of the particle and the collector, respectively.

The first term in equation 2 is the Coulomb force between two point charges placed in the particle and the collector centres. The second term is the force on the particle due to the image charge induced on the particle by the charged collector. The third term is the force caused by the charge induced on the collector by the charged particle. The image forces in equation 2 are reduced only to the first two terms of much complex infinite recurrent series.

The effect of image forces is only important when both objects are close to each other. It was shown [34], using numerical simulation, that the image forces only slightly participate in the total force when distance between the droplet and the particle for particles smaller than 3 μm . Similar results were obtained by Tripathi and Harrison, 2002 who observed a sharp decrease in the collection efficiency for small charged particles approaching an uncharged droplet. The image forces can be important for large particles, even if the particles and droplet are charged with the same polarity [34], or when either the droplet or particle is only charged to a few elementary charges [35].

The effect of the image force is only important when both objects are close to each other and for the low Coulomb numbers. Therefore, insertion of this force only slightly modifies the results of simulation. The role of the image forces is important when either the droplet or the particle is very weakly (i.e., up to a few elementary charges) charged, or uncharged at all. Thus for our calculations we assume image forces to be zero.

The aerodynamic drag force on the particle is usually presented in the following form [22]:

$$\vec{F}_A = \frac{C_d \text{Re}_p}{24} \vec{F}_S \quad (3)$$

where,

C_d is the drag coefficient,

Re_p is Reynolds number based on the particle,

\vec{F}_S is Stokes drag force.

$$\vec{F}_S = \frac{6\pi\eta_g R_p}{C_c} (\vec{u} - \vec{w}) \quad (4)$$

where,

η_g is gas viscosity,

C_c is the Cunningham slip correction factor,

\vec{u} is the gas velocity in the undisturbed region (far from collector) [33].

For the Reynolds numbers based on the particle diameter, Re_p , smaller than $2 \cdot 10^5$ the drag coefficient (C_d) can be calculated from the following equation [36]:

$$C_d = 24 Re_p^{-1} + 3.73 Re_p^{-0.5} - \frac{4.83 \cdot 10^{-3} Re_p^{0.5}}{1 + 3 \cdot 10^{-6} Re_p^{1.5}} + 0.49 \quad (5)$$

Non-dimensional parameters have been introduced in order to reduce the number of different parameters affecting the solution and to generalize the problem. All distances have been normalized with respect to the collector radius R_c , all velocities have been normalized to the gas velocity u_0 in the undisturbed region (far from the droplet), and non-dimensional time was defined as $\bar{t} = tu_0/R_c$. Equation (1) can now be written in a non-dimensional form as:

$$\frac{d\vec{w}}{dt} = \frac{C_d Re_p (\vec{u} - \vec{w})}{24 S_t} + \mathbf{G} + \frac{K_c \vec{r}}{S_t r^3} \quad (6)$$

The particle trajectories are affected by only three non-dimensional parameters. The importance of the electric forces is expressed by the Coulomb number [31]:

$$K_c = \frac{C_c Q_p Q_c}{24 \pi^2 \eta_g u_0 R_c^2 R_p} \quad (7)$$

The inertial deposition is proportional to the Stokes number, given as [31]:

$$S_t = \frac{2 C_c R_p^2 \rho_p u_0}{9 \eta_g R_c} \quad (8)$$

where ρ_p is the particle density.

The non-dimensional gravity force can be calculated from [31]:

$$\mathbf{G} = \mathbf{g} \frac{R_c}{u_0^2} \quad (9)$$

In the dimensionless form, the equation of particle motion can also be written as [32]:

$$\frac{d^2 \vec{r}}{d\bar{t}^2} = \frac{C_d R_{ep}}{24 S_t} \left(\vec{u} - \frac{d\vec{r}}{dt} \right) + \vec{g} \frac{R_p}{\mu_0^2} + \frac{K_c \vec{r}}{S_t |\vec{r}|^3} \quad (10)$$

For the purpose of the numerical solution, the vector above equation can be rewritten as a system of 2 scalar equations in the system of coordinates:

$$\frac{d^2 x}{d t^2} = \frac{C_d R_{ep}}{24 S_t} \left(u_x - \frac{dx}{dt} \right) + \frac{K_c x}{S_t r^3} \quad (11)$$

$$\frac{d^2 y}{d t^2} = \frac{C_d R_{ep}}{24 S_t} \left(u_y - \frac{dy}{dt} \right) + \frac{K_c y}{S_t r^3} + \mathbf{G} \quad (12)$$

It is assumed for simplicity that both the droplet and the particles are spherical and the flow field in the vicinity of the droplet is not disturbed by the particles.

5.3.2 Droplet trajectory

In early, simplified approaches to electro-scrubbing processes, the collector was assumed to be stationary, and in this case, the problem of particle motion could be solved relatively easy. However, advances in computational technique made it possible to include an additional vector equation of motion of the collector droplet [22]:

$$m_c \frac{d\vec{v}}{dt} = \vec{F}_{dc} + \vec{F}_e + m_c \vec{g} \quad (13)$$

Earlier theoretical models of the water scrubbing process assumed collecting droplets to be stationary. This is not correct, as the droplet falls down and its motion changes scrubbing condition. Here, it has been assumed that the droplet enters the channel with some initial velocity having only the vertical component ($v_y = v_{y0}$, $v_x = 0$, $v_z = 0$). This velocity does not remain constant as the droplet is accelerated due to the gravity and also the drag force of the flowing gas. In steady-state conditions, the horizontal component of velocity will eventually be equal to the velocity of the surrounding gas. Simulation of dust particle flow in three-dimensional space can provide much more information on the complex nature of the scrubbing process and allows determination of the space from which the particles can be captured. Both components of the droplet velocity vector satisfy the following system of differential equations [31]:

$$\frac{d\bar{v}_x}{dt} = 1 - \frac{3\rho_g}{8\rho_c} \bar{v}_c \bar{v}_x C_x \quad (14)$$

$$\frac{d\bar{v}_y}{dt} = g \frac{R_c}{u_0^2} - \frac{3\rho_g}{8\rho_c} \bar{v}_c \bar{v}_y C_x \quad (15)$$

$$\bar{v}_c = \sqrt{(1 + \bar{v}_x)^2 + \bar{v}_y^2} \quad (16)$$

Where,

ρ_g = gas density,

ρ_c = collector density,

c_x = drag coefficient depending on Reynolds number of the collector,

\bar{v}_x and \bar{v}_y are the dimensionless components of the droplet velocity (\bar{v}_c),

Here c_x depends on the Reynolds number of the collector. For Reynolds numbers $Re_c \leq 10^5$ parameter c_x can be approximated by the Kaskas equation [33]:

$$C_x = \frac{24}{Re_c} + \frac{4}{\sqrt{Re_c}} + 0.4 \quad (17)$$

5.4 Numerical simulation algorithm

The differential equations 11, 12, 14 and 15 form a simultaneous set of differential equations for the motion of dust particle and the collector. Thus these differential equations can be solved simultaneously using the fourth order Runge-Kutta algorithm for $z=0$ plane only. The trajectories of the dust particle and the collector are traced assuming some of the initial conditions as following:

1. The dust particle is initially located at point (x_0, y_0, z_0) with initial velocity equal to the velocity of the gas in horizontal direction only defined as $(u_0, 0, 0)$.
2. The collector is initially located at point $(0, 0, 0)$ with initial velocity due to gravity in vertical direction and zero velocity in horizontal direction defined by $(0, v_0, 0)$.
3. The equations of motion for the dust particles and the collector are solved simultaneously up to the collision point of both.
4. The graphs are plotted for different values of Coulomb, Stokes and Reynolds number, while changing one and keeping all others constant.
5. The graphs are plotted for $K_c=-10$ to $K_c = -100$ for different initial locations of the dust particle and different values of Reynolds number constant for a graph $Re_c=1$, $Re_c=10$ and $Re_c=100$. Here negative sign of K_c represents the opposite polarities of the particle and the droplet.
6. The variation in efficiency is plotted with respect to variation in the Coulomb number. Here efficiency is the ratio number of particles collected by the droplet to the total number of particles falling on the collector.

CHAPTER 6

RESULTS AND DISCUSSION

6.1 Particle Trajectory

The equations of motion for particle as well as the collector have been derived. Now using these equations the particle trajectories with respect to collector droplet are plotted. From the equations we know that we have three main variables which are varied and the particle motion is studied, keeping all others constant. These three variables are Coulomb number (K_c) affecting the attractive force acting on the particle due to oppositely charged collector droplet, Stokes number (St) affecting the drag force acting on the particle and finally the radius of the collector droplet (R_c) that is affecting the surface area for the dust collection.

From the equations stated we know that:

- Coulomb number (K_c) varies as the inverse of the square of the radius of the collector droplet.
- Stokes number (St) varies as the inverse of the radius of the collector the collector droplet.

Using these we have different set of conditions for which the particle trajectories are simulated.

Case 1: $R_c = 1\mu\text{m}$, $K_c = -10$ and $St = 0.1$, as shown in Figure 6-1

Case 2: $R_c = 1\mu\text{m}$, $K_c = -100$ and $St = 0.1$, as shown in Figure 6-2

Case 3: $R_c = 1\mu\text{m}$, $K_c = -10$ and $St = 1$, as shown in Figure 6-3

Case 4: $R_c = 1\mu\text{m}$, $K_c = -100$ and $St = 1$, as shown in Figure 6-4

Case 5: $R_c = 1\mu\text{m}$, $K_c = -10$ and $St = 10$, as shown in Figure 6-5

Case 6: $R_c = 1\mu\text{m}$, $K_c = -100$ and $St = 10$, as shown in Figure 6-6

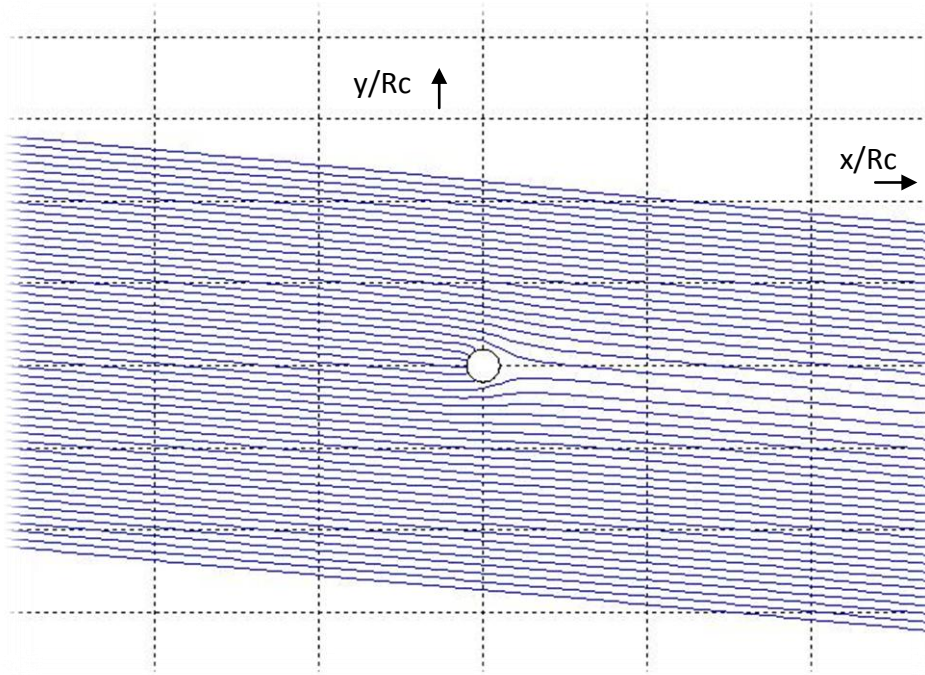


Figure 6.1: Particle trajectories in presence of oppositely charged collector when $Kc=-10$, $St=0.1$ and $Rc=1$

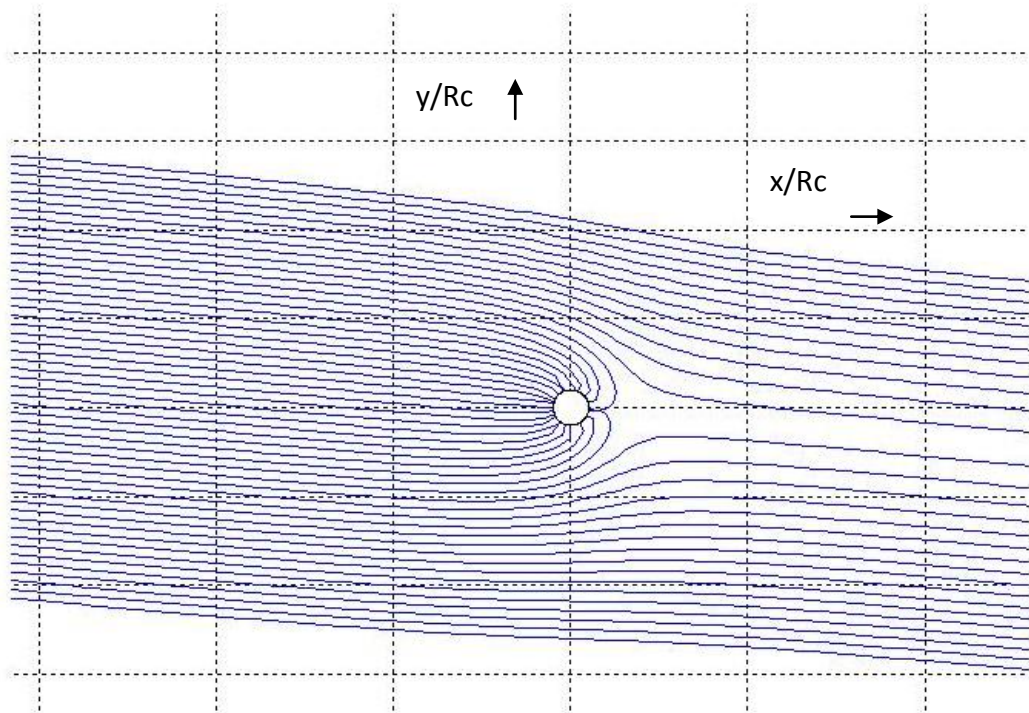


Figure 6.2: Particle trajectories in presence of oppositely charged collector when $Kc=-100$, $St=0.1$ and $Rc=1$

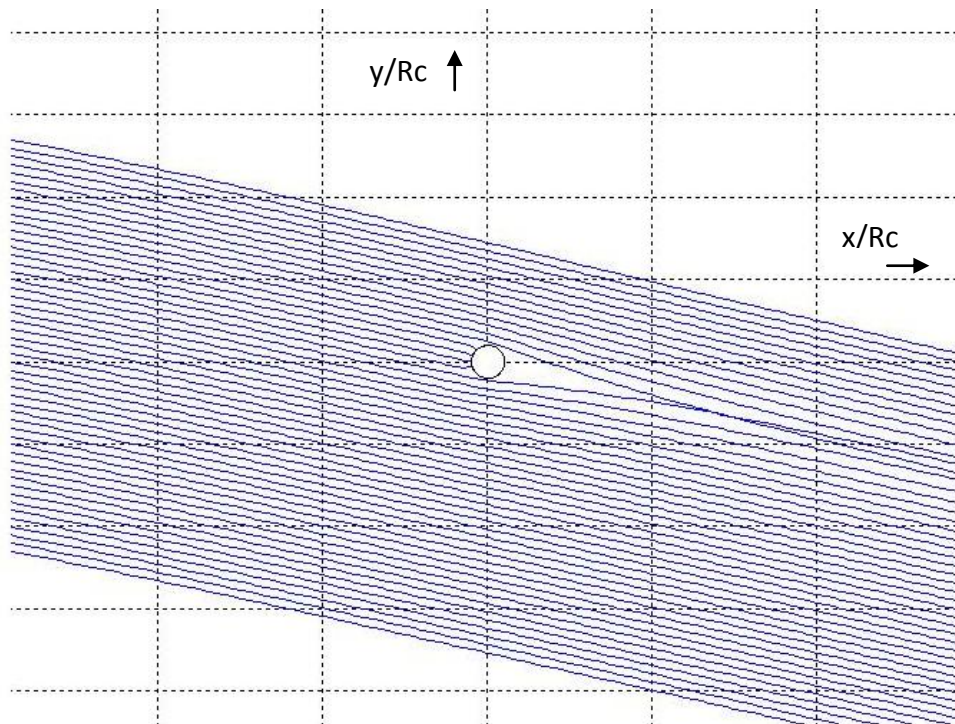


Figure 6.3: Particle trajectories in presence of oppositely charged collector when $Kc=-10$, $St=1$ and $Rc=1$

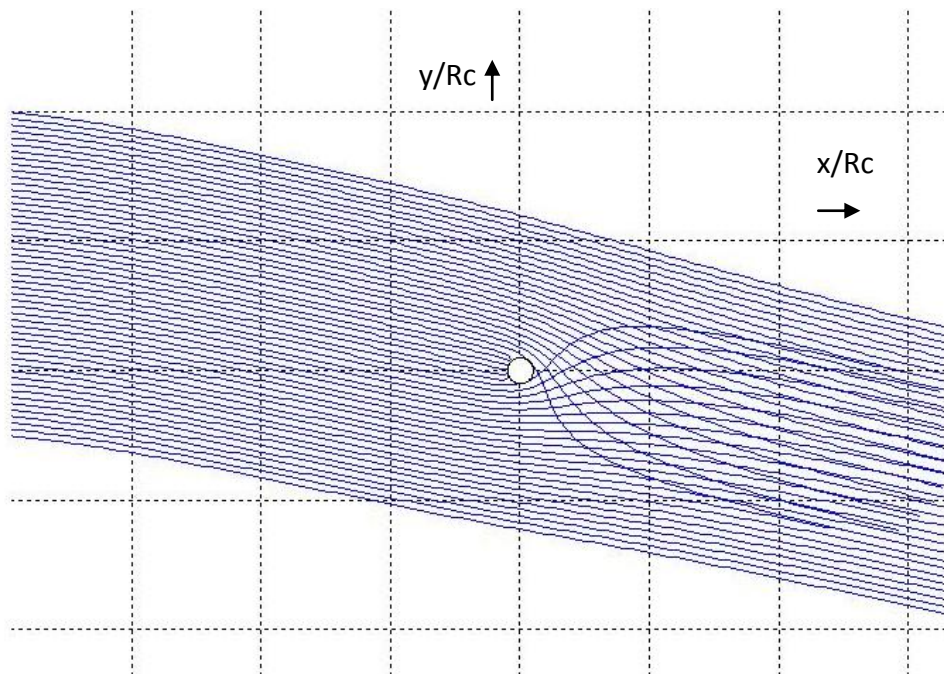


Figure 6.4: Particle trajectories in presence of oppositely charged collector when $Kc=-100$, $St=1$ and $Rc=1$

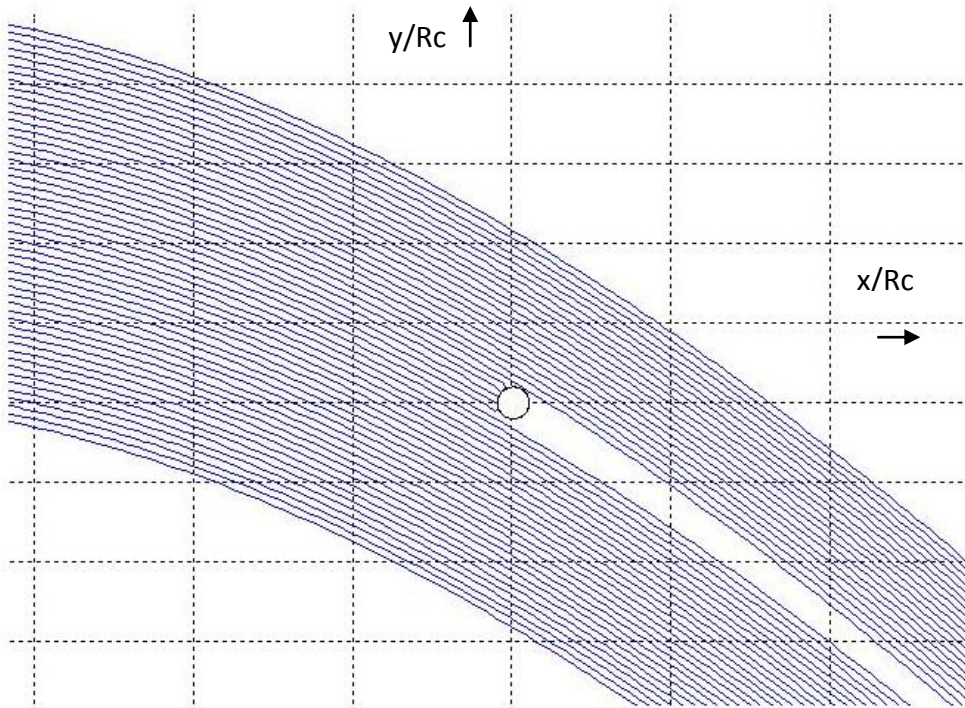


Figure 6.5: Particle trajectories in presence of oppositely charged collector when $K_c=-10$, $St=10$ and $R_c=1$

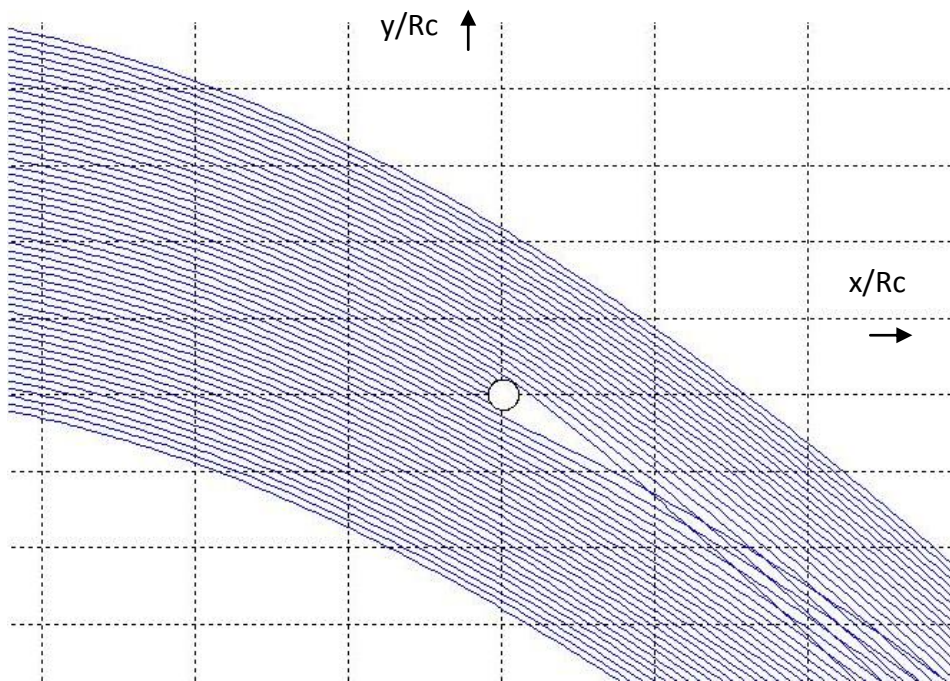


Figure 6.6: Particle trajectories in presence of oppositely charged collector when $K_c=-100$, $St=10$ and $R_c=1$

6.2 Collection Efficiency

The efficiency of the collector for a defined situation is calculated by taking the percentage number of particles collected by the collector to the total number of particles falling on the collector. There are two main parameters one of which is varied according to different situations for calculating the efficiency. These are:

1. Charge of the collector that is Coulomb number
2. Radius of the collector

These are varied when different a value of Stokes number is kept constant for a particular case (drags force).

- The Coulomb number depends on the charge as well as the radius. K_c is proportional to charge of the collector and is inversely with the square of the radius of the collector.
- The Stokes number is inversely proportional to the radius of the collector.

Using these we have different set of conditions for which the collection efficiency variation is studied with variation of one of the parameters keeping all others constant.

Case 1: Charge on the collector ($K_c = -100/R_c^2$) and Stokes number are kept constant ($St = 0.1$); collection efficiency is studied with respect to variation of collector radius for initial values only, as shown in Figure 6.7(a, b).

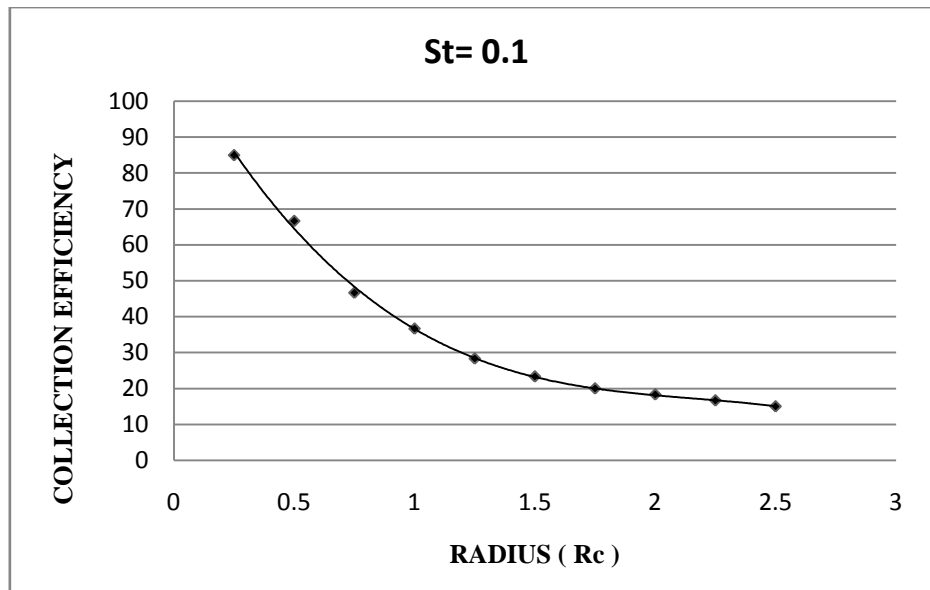


Figure 6.7(a): Radius Vs Collection efficiency at $St=0.1$

Here the efficiency decreases as the radius increases with the charge kept constant.

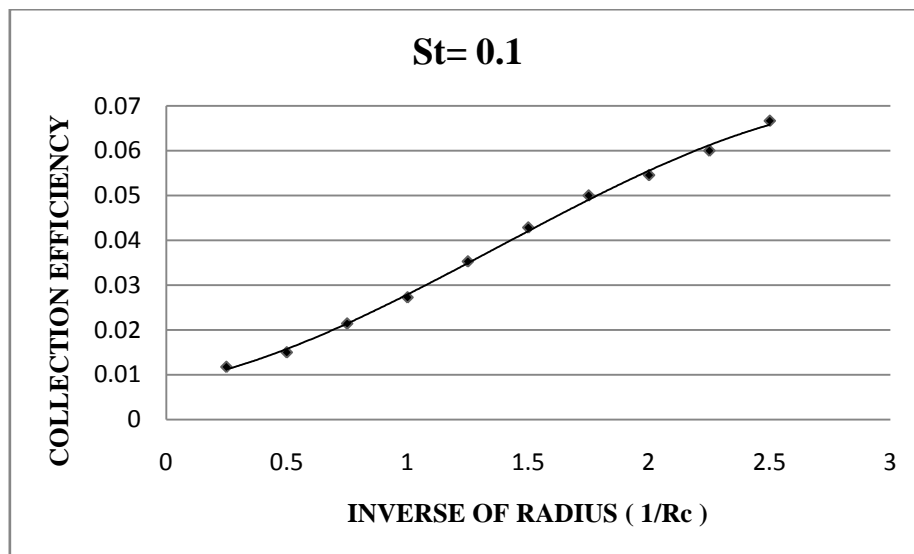


Figure 6.7(b): Inverse of Radius Vs Collection efficiency at $St=0.1$

With this Coulomb number and Stokes number value, the collector efficiency decreases with increase in collector radius. The Figure 6.7(b) shows that the collection efficiency varies as the inverse of collector radius.

Case 2: Charge on the collector ($Kc = -100/Rc^2$) and Stokes number are kept constant ($St = 0.1$); collection efficiency is studied with respect to variation of collector radius, as shown in Figure 6.8.

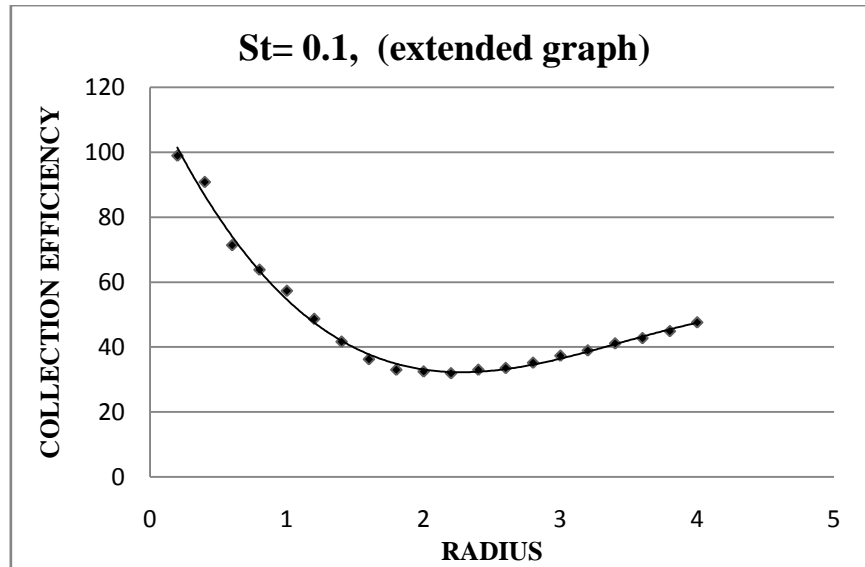


Figure 6.8: Radius Vs Collection efficiency at $St=0.1$, extended graph

The primary objective of designing electrostatic scrubber is to achieve high collection efficiency. The simulated results pictorially represent the variation of collection efficiency with respect to radius of the charged collector droplet as in Figure 6.8. This figure may be interpreted in simple words as following:

- i) Collection efficiency depends upon the electrostatic field around the charge and as the radius of the charged particle increases, the field for the given distance from the surface of charged collector droplet decreases. Thus, as the radius of charged collector droplet increases the collection efficiency decreases. This is depicted in the first quarter of the curve.
- ii) The collection efficiency is also supposed to increase with the increase in surface area of the charged collector particle. And this is depicted in the later quarter of the graph.

These two trends are opposing in nature, for the smaller radii the first trend dominates while for larger radii second trend dominates. Therefore a trade off takes place at a crossover point wherein the collection efficiency is minimum. Designers thus are to stay away from this minimum point preferably on the lower side of the radius since the gain in collection efficiency after the minimum point is not as steep as in moving on the opposite side. This work reports variation of collection efficiency with respect to radius for constant Stokes number. The future work may be directed towards studying the variation of collection efficiency with respect to keeping radius as constant. This point of minima is different for different Stokes number and may not be visible for many practical situations.

Case 3: Charge on the collector ($Kc = -100/Rc^2$) and Stokes number are kept constant ($St = 10$); collection efficiency is studied with respect to variation of collector radius, as shown in Figure 6.9.

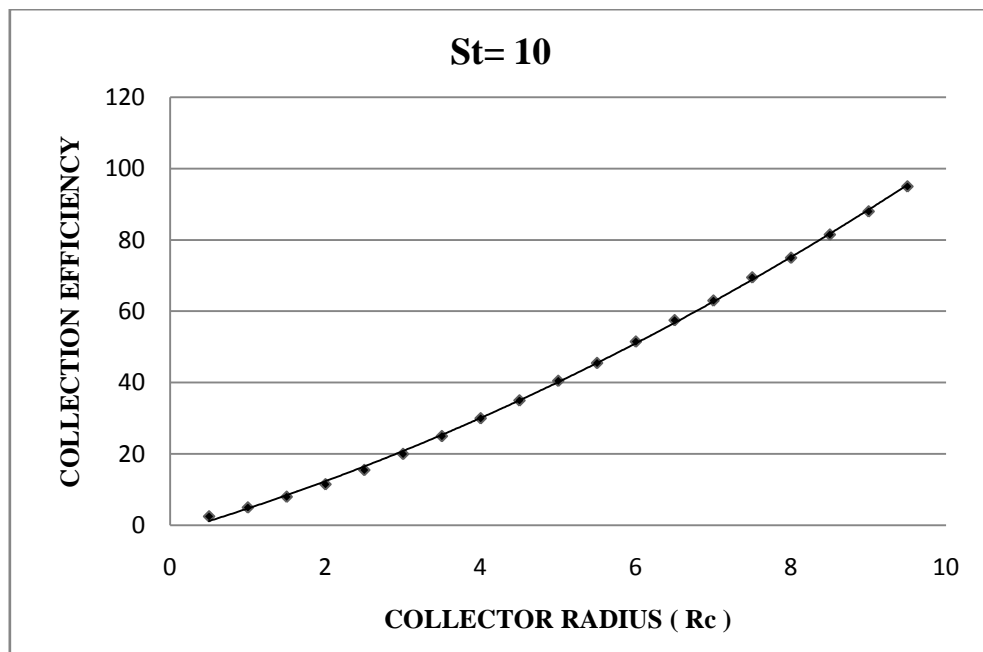


Figure 6.9: Radius Vs Collection efficiency at St=10

For the same radius and Coulomb number as in previous cases, the value of Stokes number is increased. With this greater value of Stokes number the drag force dominates as compared to the Coulomb force acting on the particle. Thus due to this, the collection efficiency increases with the increase in radius only and hence the Coulomb force can be neglected. The reason for this increase in collection efficiency can be interpreted as increase in collection surface area of the collector droplet. Thus we can say that Coulomb force does not play any role for high values of the Stokes number.

Case 4: Charge on the collector ($Kc = -10/Rc^2$) and Stokes number are kept constant ($St = 0.1$); collection efficiency is studied with respect to variation of collector radius, as shown in Figure 6.10.

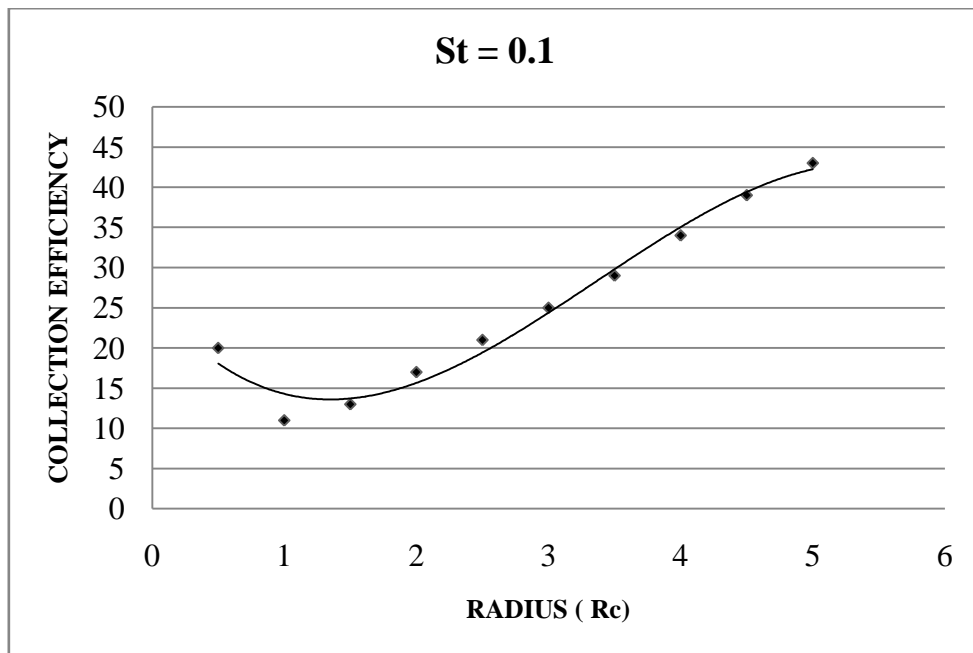


Figure 6.10: Radius Vs Collection efficiency at $St=0.1$, $Kc = -10$

With increase in collector radius, efficiency decreases initially. This is due to Coulomb effect since coulomb number varies a inverse of the square of collector radius. Since the coulomb number has very small value initially, thus its effect diminishes. Now the collection efficiency varies linearly with the increase in collection surface area.

Case 5: Collector radius ($R_c = 1\mu\text{m}$) and Stokes number are kept constant ($St = 0.1$); collection efficiency is studied with respect to variation of Coulomb number, as shown in Figure 6.11(a).

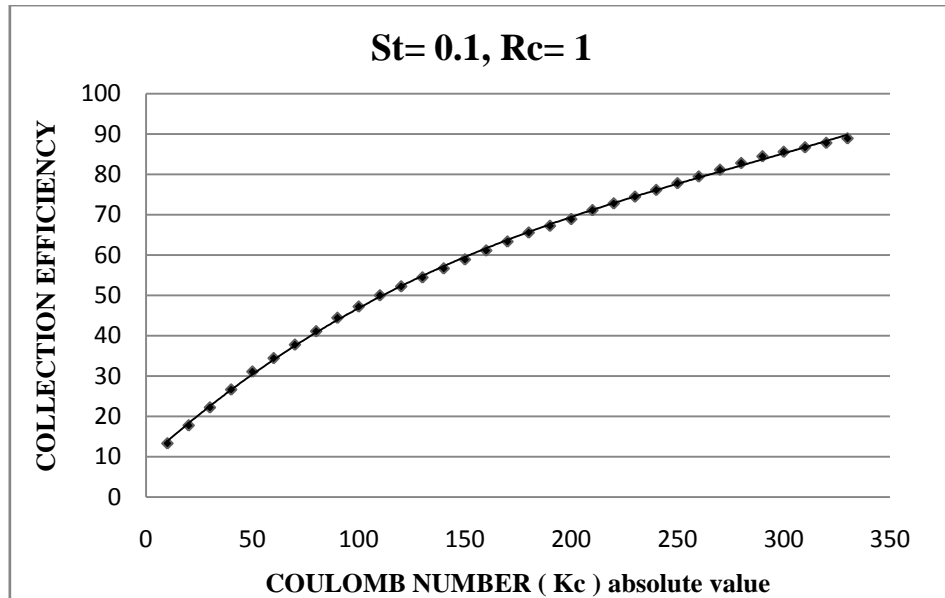


Figure 6.11(a): Coulomb number Vs Collection efficiency at $St=0.1$, $R_c=1$

Assume a condition for fixed radius of the collector and low Stokes number. Now the Coulomb number is increased. Since our collector radius is fixed, the Coulomb number can be assumed to increase due to increase in the amount of charge on the collector droplet. Thus due to increase in Coulomb number the attractive force acting on the particle due to oppositely charged collector droplet also increases. Hence this increase in Coulomb number leads to increase in collection efficiency. This increase is exponentially saturating in nature. Thus collection efficiency seems to become constant for too large values of Coulomb number with the fixed values of Stokes number and the collector radius.

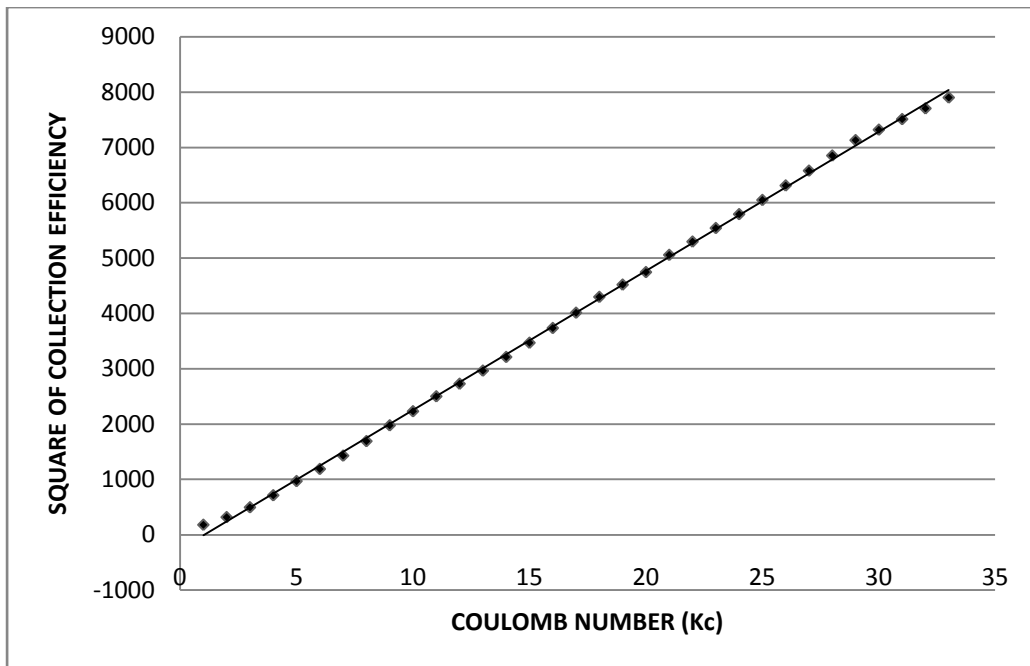


Figure 6.11(b): Coulomb number Vs square of Collection efficiency at $St=0.1$, $Rc=1$

The collection efficiency with variation of Coulomb number keeping $St=0.1$ and $R_c=0.1\text{mm}$ is as plotted in Figure 6.11(a). This variation can be studied better by plotting Coulomb number with square of collection efficiency. Figure 6.11(b) shows linear variations, thus proving that collection efficiency varies linearly with the square root of the Coulomb number.

It is clear from the above results that the collection efficiency of a scrubber system increases as the square root of the Coulomb number. We know that Coulomb number is directly proportional to the charge on the droplet and inversely proportional to the distance between the particle and collector. Thus the distance up to which the particles are collected increases as the square root of the charge on the droplet. Hence we can say that with the increase in charge, the Coulomb number increases which increases the distance to which the particles can be collected by the droplet thus increasing the collection efficiency of the system.

Case 6: Comparison of collection efficiency variation with collector radius for same Coulomb number ($Kc = -100/Rc^2$) but different Stokes number ($St = 0.1, 1, 10$), as shown in Figure 6.12.

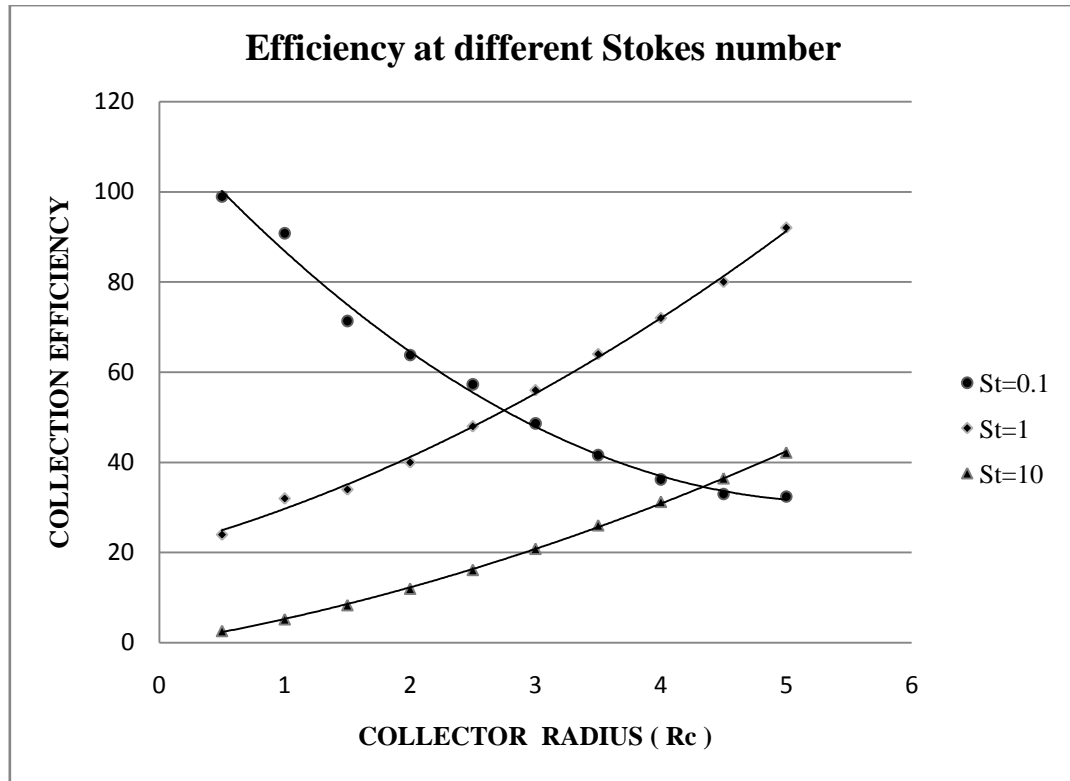


Figure 6.12: Comparing Collector radius Vs Collection efficiency at $St=0.1, 1$ and 10

From this graph we see that for this Coulomb number value, there is a decrease in collection efficiency for the very small Stokes number value. While there is an increase in collection efficiency for high Stokes number values. That is for some Stokes number only the lower quarter before the minima is visible while for some only the higher quarter is visible. And for some both the sections are clearly visible. The reasons for these trends are explained already.

Case 7: Comparison of collection efficiency variation with Stokes number for different collector radius ($R_c = 1, 2, 3$), as shown in Figure 6.13.

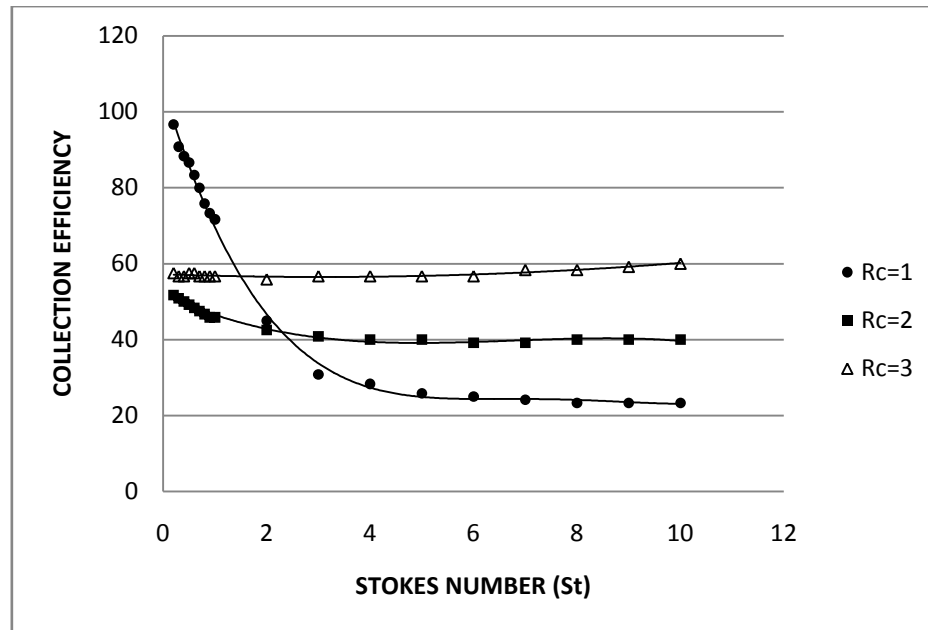


Figure 6.13: Stokes number Vs Collection efficiency

The graphs are plotted by varying the Stokes for different collector sizes keeping all other parameters constant. Thus we can see that the collection efficiency is maximum for smaller values of stokes number and decreases with increase in Stokes number. But this decrease is high for lower values of the radius and remains almost constant for higher collector radius sizes.

CHAPTER 7

CONCLUSION AND FUTURE SCOPE

7.1 Conclusion

In this thesis work, a simple numerical analysis method is proposed to plot these trajectories without using any complex numerical techniques. The two dimensional differential equations of motion for the dust particle and the collector droplet have been solved simultaneously using Runge-Kutta algorithm. Now to optimize the collection efficiency of the electrostatic scrubber in the given constrains, we have studies the effect of various parameters. Thus for this the study was carried on for different factors.

The trajectory plots help us understand the path traversed by the dust particles under given set of conditions in detail. Thus from this we can understand the working of the scrubber. Now to optimize the efficiency of the scrubber, its collection efficiency is studied parameters such as collector radius, Coulomb number and Stokes number.

When the collector radius is varied, a trade off takes place at a crossover point wherein the collection efficiency is minimum. Designers thus are to stay away from this minimum point preferably on the lower side of the radius since the gain in collection efficiency after the minimum point is not as steep as in moving on the opposite side. This point of minima is different for different Stokes number and may not be visible for many practical situations.

When the collection efficiency is studied with respect to Coulomb number we can safely conclude that with the increase in charge, the Coulomb number increases which increases the distance to which the particles can be collected by the droplet thus increasing the collection efficiency of the system.

For variation in Stokes number, the collection efficiency decreases with the increase in Stokes number for given set of conditions. But this decrease is high for lower values of the radius and remains almost constant for higher collector radius sizes.

Thus these efficiency graphs plotted will help in designing the scrubber for the given set of conditions by studying the effect of each of them individually.

7.2 Future Scope

The particle trajectories can be studied by considering other forces to a greater detail since this method does not include any complexity. For solving these equations Runge-Kutta was one technique, other numerical techniques can also be used for solving these equations. Our assumption here was that mass of the droplet does not change although it practically does, thus the effect of change of mass and momentum can be carried out further. The effect of other parameters such as air velocity, basset forces, Reynolds number, particle density etc. can also be studied in detail for the better understanding and design of the scrubber system. The results obtained here use the supposed assumptions; these results need be verified with the experimental results for similar parameters.

REFERENCES

- [1] Gerald T. Joseph; David S. Beachler, "Scrubber Systems Operation Review," APTI Virtual Classroom, U.S. Environmental Protection Agency, 1998, can be sited at:
http://yosemite.epa.gov/oaqps/EOGtrain.nsf/DisplayView/SI_412C_0-5?OpenDocument
- [2] "SI:412B Electrostatic Precipitator Plan Review," APTI Virtual Classroom, U.S. Environmental Protection Agency, can be sited at:
http://yosemite.epa.gov/oaqps/EOGtrain.nsf/DisplayView/SI_412B_0-5?OpenDocument
- [3] Jaworek A.; Krupa A., "ELECTROSTATIC SCRUBBING" can be sited at:
www.imp.gda.pl/ehd/el_scrub.html
- [4] Pilat M.J., "Electrostatic Aerosol Scrubber and Method of operation", United States Patent, 4,193,774, 18 March, 1980.
- [5] Klugman W.L., Kosmider J., "Method for Electrostatic removal of Particulate from a gas stream", United States Patent, 3,958,958, 25 May, 1976.
- [6] Waldron R.A., "Electric Forces", Radio and Electronic Engineer, vol.51(11-12), pp.553-560, 1981.
- [7] Metzler P., Weib P., Buttner H. and Ebert F., "Electrostatic enhancement of the dust separation in a nozzle scrubber", J. Electrostatics, vol.42(1-2), pp.123-141, 1997.
- [8] Flagan R.C.; Seinfeld J.H., "Fundamentals of Air Pollution Engineering", Prentice Hall, New Jersey, 1988.
- [9] Talbot L.; Cheng R.K.; Schefer R.W.; Willis D.R., "Thermophoresis of Particles in a Heated Boundary Layer", J. Fluid Mech., pp.737-758, 1980.
- [10] Derjaguin B.V.; Yalamov Y., "The Theory of Thermophoresis and Diffusiophoresis of Aerosol Particles and Their Experimental Testing", Pergamon Press, New York, 1972.
- [11] Fuchs N.A., "Mechanics of Aerosols", Pergamon Press, New York, 1964.
- [12] Price R.H.; Wood J.E.; Jacobsen S.C., "The Modelling of Electrostatic Forces in Small Electrostatic Actuators", IEEE Transactions, pp.131-135, June 1988.

- [13] Reynolds W.C.; Perkins H.C., “Engineering Thermodynamics”, McGraw-Hill, New York, 1977.
- [14] Friedlander S.K., “Smoke, Dust and Haze-Fundamentals of Aerosol Behavior”, Wiley, New York, 1977.
- [15] Crawford M., “Air Pollution Control Theory”, McGraw-Hill, New York, 1976.
- [16] Tuekolsky; Vetterling; Flannery, “Numerical Recipes in C, Cambridge University Press. 1992.
See www.nr.com for free pdf version.
- [17] Storey B.D., “Numerical Methods for Ordinary Differential Equations” can be sited at:
http://icb.olin.edu/fall_02/ec/reading/DiffEq.pdf
- [18] Ascher U.M.; Petzold L.R., “Computer Methods for Ordinary Differential Equations and Differential-Algebraic Equations,” SIAM, Philadelphia, 1998.
- [19] Wiley J.; Sonce, “An Introduction to Numerical Methods and Analysis,” Epperson, 2002.
- [20] MATLAB Product Documentation can be sited at:
<http://www.mathworks.com/help/techdoc/ref/ode23.html>
- [21] P. Metzler; P.Weiß; H. Büttner; F. Ebert, “Electrostatic enhancement of the dust separation in a nozzle scrubber,” J. Electrostatics, vol.42, no.1–2, pp.123–141, 1997.
- [22] Jaworek A.; Balachandran W.; Krupa A.; Kulon J.; Lackowski M., “Wet Electroscrubbers for State of the Art Gas Cleaning,” Environmental Science & Technology, vol.40, no.20, pp.6197-6207, 2006.
- [23] Pilat M.J.; Jaasund S.A.; Sparks L.E., “Collection of Aerosol Particles by Electrostatic Droplet Spray Scrubber,” Environmental Science & Technology, vol.8, no.4, pp 360-362, Apr. 1974.
- [24] George H.F.; Poehlein G.W., “Capture of Aerosol Particles by Spherical Collectors: Electrostatic, Inertial, Interception, and Viscous Effects,” Environmental Science & Technology, vol.8, no.1, pp.46-49, Nov. 1974.
- [25] Nielsen K.A.; Hill J.C., “Collection of Inertialess Particles on Spheres with Electrical Forces,” Ind. Eng. Chem., Fundam., vol.15, no.3, pp.149-156, 1976.

- [26] Nielsen K.A.; Hill J.C., "Capture of Particles on Sphere by Inertial and electrical Forces," *Ind. Eng. Chem., Fundam.*, vol.15, no.3, pp.157-163, 1976.
- [27] Wang H.C.; Stukel J.J.; Leong K.H., "Charged particle Collection by an Oppositely Charged Accelerating Droplet," *Aerosol Science and technology*, pp.409-421, Jan. 1986.
- [28] Price R.H.; Wood J.E.; Jacobsen S.C.; "The Modelling of Electrostatic Forces in Small Electrostatic Actuators," *IEEE*, pp.131-135, 1988.
- [29] Kraemer H.F.; Johnstone H.F., "Collection of Aerosol Particles in Presence of Electrostatic Field," *Industrial Engineering and Chemistry*, vol.47, no.12, pp.2426-2434, Dec. 1995.
- [30] Adamaik K.; Jaworek A.; Krupa A., "Deposition of Aerosol Particles on a Charged Spherical Collector," *Journal of Electrostatics*, vol.40, pp.443-448, 1997.
- [31] Adamaik K.; Jaworek A.; Krupa A., "Deposition efficiency of dust Particles on a Single, Falling and charged water Droplet," *IEEE Transactions on Industry Applications*, vol.37, no.3, pp.743-750, May/June 2001.
- [32] Jaworek A.; Adamiak K.; Krupa A., "3D Model for Trajectories of Airborne Particles near a Charged Spherical Collector," *Third International Conference on Multiphase Flow*, June 8-12, 1998.
- [33] Jaworek A.; Krupa A.; Adamaik K., "Submicron Charged Dust Particles Interception by charged Drops," *IEEE Transactions on Industry Applications*, vol.34, no.5, pp.985-991, Sep./Oct.1998.
- [34] Jaworek A.; Adamiak K.; Balachandran W.; Krupa A.; Castle P.; Machowski W., "Numerical Simulation of Scavenging of Small Particles by Charged Droplets," *Aerosol Science and Technology*, vol.36, pp.913-924, Nov. 2002.
- [35] Tinsley B.A.; Rohrbaugh R.P.; Hei, M.; Beard K. V., "Effects of image charges on the scavenging of aerosol particles by cloud droplets and on droplet charging and possible ice nucleation processes," *J. Atmos. Sci.*, vol.57, pp.2118-2134, 2002.
- [36] Brauer H.; Sucker D., "Flow about plates, cylinders and spheres," *Int. Chem. Eng.*, vol. 18, pp. 367-374, 1978.

Appendix A

The following program is used to plot the particle trajectories with respect to a collector droplet at the centre. The program was designed and simulated using MATLAB computing software.

```
% main program for xy
```

```
global St Cd Rep Kc g Rc Uo u Cc Rp p n G rx ry a1 a2 Vy Rec
```

```
deposite(m)=0;
```

```
input(m)=0;
```

```
Uo=5;          % gas velocity in undisturbed region
```

```
Rc = 1;        % collector radius
```

```
Rp = .01;
```

```
Kc = -100/(Rc^2); % coloumb number
```

```
%Rep= (p*Uo*2*Rp)/mu
```

```
Rep = 2000*Rp; % reynolds number based on the particle
```

```
%Rec= (p*V*2*Rc)/mu
```

```
Rec=100*Rc;    % reynolds number of the collector
```

```
St=10/Rc;     % stokes number
```

```
g =-9.8;      % force of gravity
```

```
Cd = 24*(Rep^-1)+3.73*(Rep^-0.5)-((4.83*(10^-3)*(Rep^0.5))/(1+3*(10^-6)*(Rep^1.5)))+0.49;
```

```
    % non-stokian drag coefficient for Rep< 2*10^5
```

```

% now calculating co-ordinates of droplet in (m,n)
Vy = g*Rc/Uo^2;

c1=-40;
c2=5;
rx=c1;      % rx is the initial x co-ordinates of the particle
            % ry is the initial y co-ordinates of the particle
for ry=c2:.1:35;
input(m)=input(m)+1;

tspan = [0:0.1:15];      % time span to study

a0 = [rx Uo ry Vy 0 0 0 Vy];      %initial values

[t,a]= ode45('may10_1',tspan,a0);
                                % using runge-kutta method

% t gives time vector
% a gives solution matrix; where each column represents vector for its
% corresponding variable

a1=a(:,1);  % a1 gives solution vector for dr/dt(x co-ordinates)
a2=a(:,2);  % a2 gives solution vector for d2r/dt2(x co-ordinates)

x=a(:,5);
y=a(:,7);

k3=size(x);
k1=x(k3(1,1),1);
k2=y(k3(1,1),1);
[latc,lonc] = scircle1(k1,k2,Rc);

```

```

b1=a(:,3); %b1 gives solution vector for dr/dt(y co-ordinates)
b2=a(:,4); %b2 gives solution vector for d2r/dt2(y co-ordinates)

% now calculating the relative difference between the two points
% that is radial distance between particle and collector

t1 = a1-x;
t2 = b1-y;
d1=size(t1);

Rcc=Rc+abs(k2);
for i=1:1:d1(1,1)

    if (((abs(t1(i,1)))^2+(abs(t2(i,1)))^2)^0.5<=Rcc)
        deposite(m)=deposite(m)+1;
        l=i;
        while l<=d1(1,1)

            t1(l,1)=0;
            t2(l,1)=0;
            l=l+1;
        end
    break
end
end

if (rx==c1&&ry==c2)
figure(m)
plot(t1,t2)
grid

```

```
axis equal
xlabel(' x co-ordinates')
ylabel(' y co-ordinates')
title('trajectory of particle with respect to the droplet')
else
    figure(m)
    line(t1,t2)
end

clear('tspan','a0','t','a','a1','x','bo','b','b1','y','t1','t2');
end
hold all
fill(latc, lonc,'w')
end

deposite
input
```

PUBLICATIONS

1. Dr. Mandeep Singh and Kriti Jain, “Determining trajectory of charged particle in electrostatic scrubber - A simplified approach,” paper accepted to be published in International Journal of Electronics Engineering.
2. Dr. Mandeep Singh and Kriti Jain, “Variation of particle collection efficiency of electrostatic scrubber with Coulomb number,” paper accepted to be published in International Journal of Electronics Engineering.
3. Dr. Mandeep Singh and Kriti Jain, “Effect of collector radius on collection efficiency of electrostatic scrubber,” paper accepted to be published in International Journal of Electronics Engineering.
4. Dr. Mandeep Singh and Kriti Jain, “A novel method for establishing collection efficiency of electrostatic scrubber as a function of stokes number,” paper accepted to be published in International Journal of Electronics Engineering.